From wind to hydrogen: mapping the competitiveness of hybrid offshore configurations in the Mediterranean Sea

frontiers in Energy Research

TYPE Original Research
PUBLISHED 20 March 2026
DOI 10.3389/fenrg.2026.1765111

OPEN ACCESS

EDITED BY
Muhammad Aziz,
The University of Tokyo, Japan

REVIEWED BY
Sudhakar Kumarasamy,
Universiti Malaysia Pahang, Malaysia
Davoud Ghahremanlou,
Memorial University of Newfoundland, Canada
Honglin Li,
University of North Texas at Dallas, United States

*CORRESPONDENCE
Viola De Clerck,
viola.declerck@polito.it

RECEIVED 10 December 2025
REVISED 31 January 2026
ACCEPTED 17 February 2026
PUBLISHED 20 March 2026

CITATION
De Clerck V, Petracca E, Joyo FH, Bacan A, Mangia G, Nikolakakos C, Radulovic G, Marques JF, Dimeas A, Groppi D, Garcia DA, Magni GU, Gorr-Pozzi E and Bracco G (2026) From wind to hydrogen: mapping the competitiveness of hybrid offshore configurations in the Mediterranean Sea.
Front. Energy Res. 14:1765111.
doi: 10.3389/fenrg.2026.1765111

From wind to hydrogen: mapping the competitiveness of hybrid offshore configurations in the Mediterranean Sea

Viola De Clerck[1]*, Ermando Petracca[1], Farhan Haider Joyo[2], Andro Bacan[3], Gabriele Mangia[1], Christos Nikolakakos[4], Gorica Radulovic[5], João Francisco Marques[6], Aris Dimeas[4], Daniele Groppi[7], Davide Astiaso Garcia[2], Gabriele Umberto Magni[2], Emiliano Gorr-Pozzi[1] and Giovanni Bracco[1]

[1]Marine Offshore Renewable Energy Lab (MOREnergy Lab) - Department of Mechanical and Aerospace Mechanical and Aerospace Engineering (DIMEAS), Politecnico di Torino, Turin, Italy, [2]Department of Electrical and Energy Engineering, Sapienza University of Rome, Rome, Italy, [3]Energy Institute Hrvoje Požar (EIHP), Zagreb, Croatia, [4]Institute of Communication and Computer Systems (ICCS), National Technical University of Athens (NTUA), Athens, Greece, [5]ENVPRO, Podgorica, Montenegro, [6]EDP NEW, Lisbon, Portugal, [7]Department of Planning, Design, Technology for Architecture, Sapienza University of Rome, Rome, Italy

Offshore wind is central to decarbonisation, yet its deployment in the Mediterranean Sea is increasingly constrained by grid limitations and curtailment. This study presents a geospatial techno-economic competitiveness assessment of offshore wind and hybrid offshore wind-hydrogen systems across the Mediterranean basin. Results show that optimal grid-connected offshore wind configurations achieve a LCOE of 48.4/MWh, while hybrid Power-to-X configurations reach a minimum LCOH (expressed in energy-equivalent terms) of 81.4/MWh. Under favorable market conditions, hybrid systems can achieve positive net present values, with a minimum payback time of 11 years, highlighting a strong dependence of economic performance on price scenarios. Power-to-X solutions, in particular hybrid wind-hydrogen systems that convert part of the offshore wind output via electrolysis, offer an alternative route to valorize offshore wind beyond direct grid injection. The analysis evaluates hybrid configurations in which 10%–90% of the wind farm capacity is allocated to on-site hydrogen production, compared against a conventional electricity-to-grid baseline. The assessment spans diverse Mediterranean locations and adopts the levelised cost of hydrogen as the main performance indicator to compare hybrid and stand-alone electricity-export setups, alongside complementary economic metrics. Results indicate that, when considering pure cost minimization, the grid-only scenario systematically delivers the lowest levelised cost across all assessed locations. However, sensitivity analysis to electricity and hydrogen market prices shows that hybrid configurations can become economically attractive under moderate-to-favorable conditions, despite higher levelised costs. Overall, the findings demonstrate that while offshore wind-hydrogen systems are not cost-optimal under current baseline assumptions, they may represent a viable future strategy to unlock offshore renewable potential in regions

facing grid integration constraints and to support long-term hydrogen market development and decarbonisation objectives in the Mediterranean context.

KEYWORDS

geospatial modeling, green hydrogen, hybrid energy systems, mediterranean energy transition, offshore wind, power-to-X, techno-economic analysis

1 Introduction

Offshore wind is emerging as a key pillar of the EU strategy for a secure, decarbonized and sovereign energy system, complementing solar PV and onshore wind by exploiting still-underused marine resources (IPCC, 2022; International Energy Agency, 2019; International Renewable Energy Agency, 2019; European Commission, 2020a). Its growing feasibility, driven by technological progress and cost reductions, has prompted EU policies to promote interconnected offshore grids and harmonized Marine Spatial Planning (MSP), so that environmental externalities on marine ecosystems, seabeds and avian routes are managed through ecosystem-based, socially accepted siting decisions that balance ecological, economic and social objectives (EU, 2014; Bailey et al., 2014; Copping et al., 2024; Chen et al., 2025; United Nations Global Compact, 2021). Over the past decade, several European initiatives have advanced the integration of MSP and offshore renewable energy, improving spatial allocation, stakeholder engagement, and multi-use synergies. The EU MSP Platform provides Member States with tools, best practices, and guidance for implementing MSP in line with EU directives (European Commission, 2025a). Projects such as THAL-CHOR I and II, MAESTRALE, ORECCA, BlueDeal, MarinePlan and the Pelagos Forum have developed methodologies, decision support systems and governance frameworks for coordinating Blue Energy deployment and marine conservation across the Mediterranean and other European seas (Oceanography Center, University of Cyprus, 2025; European Commission, 2025b; 2012; WestMED Initiative, 2023). Beyond spatial optimization, MSP frameworks are increasingly coupled with techno-economic and environmental indicators, enabling multi-criteria evaluation of offshore wind potential. For instance, GIS-based methods such as automated visual impact assessment contribute to refining site-selection procedures into spatial decision tools (Maslov et al., 2017). Within this context, the SPOWIND (Spatial Planning for Offshore Wind Industry Development) project specifically addresses Mediterranean challenges by developing a WebGIS tool and data hub that combine MSP, techno-economic analysis, and transnational cooperation to support offshore wind planning (Interreg Euro-MED, 2025). Across the Mediterranean, the translation of EU-level mandates into national frameworks remains highly fragmented, with large differences in how NECPs and TSO development plans are aligned. This heterogeneity in EEZ planning, concessions and licensing constitutes a major non-technical barrier to investment; the national regulatory and planning landscape is summarised in Supplementary Table S1.

1.1 Offshore wind development and design considerations

Because the Mediterranean bathymetry deepens rapidly outside narrow continental shelves, fixed-bottom foundations are geographically confined, whereas floating systems unlock the offshore wind resource where the most productive cells concentrate. Compared with offshore floating solar attractive for niche e-fuel and shortsea refuelling concepts but constrained by diurnal generation and lower areal power density offshore wind provides higher full-load hours and a more continuous input for electrolysis, while extreme design conditions are driven by mid-latitude storms and occasional Mediterranean tropical like cyclones rather than Mediterranean tropical-like cyclones (Kaur et al., 2025; Ricchi, 2025). Furthermore, recent advances in turbine and foundation technologies have enabled offshore wind projects to scale in capacity and expand into deeper waters (Soukissian et al., 2017). Floating offshore wind has emerged as a crucial innovation, while the deployment of 10–15 MW class turbines has improved energy capture and reduced the number of units required per project (Petracca et al., 2024). Improvements in fixed-bottom structures and offshore transmission systems, including both high-voltage alternating current (HVAC) and high-voltage direct current (HVDC) transmission technologies, further support the integration of remote offshore resources into national grids (Onea and Rusu, 2022). In the Mediterranean Sea, these developments are met with region-specific constraints, including limited shallow-water areas, moderate wind conditions, and significant bathymetric variability. Previous studies have emphasised the importance of detailed engineering optimisation in this region, given the strong influence of turbine rating, spacing, layout geometry, and transmission design on the techno-economic feasibility of offshore wind (Gao et al., 2024). An appropriate representation of these design parameters is therefore a prerequisite for any credible assessment of Mediterranean offshore wind potential, whether in pure electricity-export or hybrid configurations.

1.2 Hybrid offshore wind-hydrogen systems

Alongside conventional offshore wind deployment, hybrid wind-to-hydrogen systems have gained increasing attention for their ability to convert part of the electrical output into green hydrogen via electrolysis, either offshore or nearshore. While this study focuses on the Mediterranean region, several export-oriented projects of hubs involving the coupling of wind energy and hydrogen production are emerging in North-Sea and North America Copenhagen Infrastructure Partners (2022), U.S. Department of Energy, Office of Clean Energy Demonstrations (2026). In the North Sea, hydrogen production is increasingly

framed within a highly interconnected infrastructure, supported by planned pipeline corridors linking offshore wind resources with industrial demand centers in Germany and continental Europe AquaDuctus Offshore/GASCADE Gastransport GmbH (2026). Likewise, Atlantic Canada, particularly Newfoundland, is developing large-scale wind-to-hydrogen projects explicitly aimed at exporting renewable fuels to Europe, leveraging abundant wind resources and direct maritime access to international markets. These initiatives underline the strategic role of hydrogen as an export commodity rather than solely a domestic energy carrier Timalsina and Ghahremanlou (2024). Compared to these regions, Mediterranean hybrid offshore wind–hydrogen hubs face distinct market and infrastructure conditions, yet they pursue similar objectives related to connectivity, diversification of energy supply, and integration into international hydrogen corridors.

Indeed, these systems can reduce curtailment, provide operational flexibility by accessing both electricity and hydrogen markets, and diversify revenue streams, which is particularly relevant under volatile electricity prices or limited grid access (Santos et al., 2024; Loisel et al., 2015). This flexibility can also support downstream uses beyond the power sector, including decentralised maritime refuelling concepts for small ferry routes via hydrogen-derived electrofuels (Kaur et al., 2025). Multiple techno-economic assessments, mainly focused on North Sea contexts, indicate that such configurations may become cost-competitive when hydrogen prices exceed about 3/kg or when power export is constrained by grid congestion or distance-to-shore limitations (Rogeau et al., 2023), thereby helping to decouple energy supply from grid availability (Kumarasamy et al., 2025). Broader energy-systems literature highlights that Power-to-X (PtX) integration enables long-duration storage and sector coupling, enhancing energy security and flexibility beyond conventional electricity-only delivery models (Breyer et al., 2018). Converting offshore wind into storable chemical carriers such as hydrogen or ammonia provides temporal arbitrage and export opportunities, which is particularly important for regions aiming to position themselves as energy exporters (International Renewable Energy Agency (IRENA), 2022; Blanco et al., 2021). However, many existing studies rely on simplified infrastructure assumptions or fixed electrolyser sizing and often neglect the co-optimization of wind-farm parameters such as turbine rating, spatial density, mooring technology, and electrical architecture (Castro-Santos et al., 2021). Only a limited number of works explore a continuous range of hydrogen allocation shares across spatial domains, and most analyses remain geographically concentrated in Northern European waters, where shallow seabeds, dense grid interconnections and mature O&M infrastructure differ markedly from Mediterranean conditions. The Mediterranean context introduces distinct technical and socio-political drivers that can make hybrid offshore configurations particularly attractive. Steep bathymetric gradients require floating platforms, which increase capital and operational costs but unlock extensive deep-water wind resources (Faraggiana et al., 2024). At the same time, several countries in the region experience transmission constraints, especially in remote coastal or insular areas where onshore grid reinforcement may be costly or delayed (Zaiter et al., 2025). In such settings, allocating part of the wind output to hydrogen production can relieve system stress and enable earlier deployment, while offshore PtX solutions reduce land-use competition and may encounter fewer permitting and social-acceptance barriers than onshore projects (Avesani, 2025). Beyond infrastructure bottlenecks, the push toward green hydrogen is increasingly shaped by regulatory, environmental and strategic imperatives. The EU Hydrogen Strategy and REPowerEU explicitly promote offshore wind as a preferred source for electrolytic hydrogen that meets renewable certification criteria (European Commission, 2020b). Although cost parity with fossil-derived hydrogen remains challenging in the near term, offshore-based production supports sustainability and energy-autonomy objectives, avoids land scarcity issues associated with solar-PV electrolysis coupling, and aligns with emerging taxonomy and carbon-accounting frameworks relevant for domestic use and export (Glenk and Reichelstein, 2019). For coastal industrial clusters, ports and shipping corridors, offshore hydrogen hubs could therefore underpin emerging clean-fuel supply chains. In light of these factors, techno-economic assessments of wind-to-hydrogen integration must move beyond static Levelised Cost of Energy (LCOE), Levelised Cost of Hydrogen (LCOH), Net Present Value (NPV) or simple Pay-Back Time (PBT) benchmarks (D'Adamo et al., 2025), and explicitly account for grid constraints, infrastructure feasibility and regulatory conditions that shape the bankability of certified renewable hydrogen in Europe (EU, 2023a; EU, 2023b; EU, 2025). Especially in the Mediterranean, where hydrogen uptake may be driven by industrial decarbonisation, maritime bunkering and cross-border trade, identifying geo-economically viable hybrid zones requires integrative spatial analyses that couple resource assessment, technology performance and infrastructure constraints. The existing literature therefore leaves at least the following gaps: (i) the lack of spatially explicit techno-economic assessments of hybrid wind–hydrogen systems at Mediterranean basin scale; (ii) the limited exploration of hydrogen-conversion fractions and electrolyser sizing across heterogeneous sites; and (iii) the absence of consistent co-optimisation between wind-farm design variables and Power-to-X sizing under coherent scenario assumptions. Two additional gaps are critical for floating-dominated basins: (iv) the limited propagation of substructure-dependent, motion-affected energy yield into basin-scale cost maps, despite evidence that platform dynamics can shift mean power and wake behaviour (Duan et al., 2025); and (v) the scarce integration of certification-driven constraints (e.g., additionality and temporal matching) into spatial LCOH estimates, which can materially affect feasible operating profiles and costs (EU, 2023a; EU, 2023b; EU, 2025). This work addresses these gaps by coupling basin-wide spatial screening with technology-driven productivity modelling (including floating substructure effects), a large design space of farm layouts and spacings, and a consistent electricity-to-hydrogen costing layer aligned with national scenario envelopes.

1.3 Present paper contributions

This study addresses the identified gaps through an integrated techno-economic framework tailored to Mediterranean offshore conditions. The workflow produces basin-scale, spatially explicit competitiveness maps for offshore wind and wind-to-hydrogen pathways, thus closing the current lack of Mediterranean-wide, site-resolved assessments for hybrid systems. The modelling chain treats farm productivity as a technology-driven outcome rather

10.3389/fenrg.2026.1765111

than an input. Productivity look-up tables embed wind-farm design choices (turbine rating, farm size, spacing and internal electrical topology) and propagate substructure-dependent performance into the spatial energy and cost layers, capturing motion-affected yield for floating concepts and linking these effects directly to cost competitiveness. The same spatial productivity basis feeds the hydrogen costing layer, ensuring that spatial variability in energy yield translates consistently into spatial variability in hydrogen cost metrics. The analysis then explores electrolyser sizing and conversion fractions across heterogeneous sites by spanning electrolyser capacities from 10% to 90% of wind-farm rated power. A coherent optimisation logic couples wind-farm design variables and Power-to-X sizing under consistent scenario assumptions, avoiding decoupled design steps and enabling a structured comparison of competing configurations. Finally, the framework maintains alignment with certification-driven constraints for renewable fuels of non-biological origin (additionality and temporal matching) and frames their implications for feasible operating profiles and spatial hydrogen-cost estimates as a priority extension of the present results (EU, 2023a; EU, 2023b; EU, 2025). The economic layer combines levelised costs with investment indicators, including net present value and payback time, over a range of electricity and hydrogen price conditions. This structure identifies price thresholds and market combinations that shift hybrid wind–hydrogen solutions from systematically dominated options to competitive alternatives in specific Mediterranean zones.

The paper is structured as follows: The methodology section first presents the full modeling framework in Section 2, including spatial eligibility analysis, wind-farm configuration, hybrid scenario evaluation (with different electrolyser sizes), and definitions of the economic analysis and metrics. Section 3 then examines the performance of the optimal wind farm and corresponding hybrid designs under various electricity and hydrogen price conditions. Section 4 summarises the main findings and their implications for future offshore development in the Mediterranean, while also detailing study limitations and potential future works.

2 Materials and methods

In order to quantify the contribution of offshore wind and its power-to-X potential to the Mediterranean energy system, this section presents the modelling framework employed to assess both electricity generation and hydrogen production. The analysis considered direct electricity delivery as well as multiple configurations involving partial conversion to green hydrogen via a hybrid, centralized offshore electrolysis scheme. Associated economic indicators are computed, including the LCOE for the EtG case, as well as for the hybrid configurations, and the NPV and PBT to support broader economic evaluation and enable consistent comparison across scenarios. The methodology is applied to previously identified suitable areas, delineated through maritime spatial analysis. An overall total of 378 configurations (see Table 1) are examined to reflect current trends in offshore wind development. Wind turbines with rated capacities of 10 MW and 15 MW are considered, deployed on monopile foundations in shallow waters (<60 m) and on floating platforms in deeper areas (<60 m). Representative wind farm capacities of 0.99, 1.5, and 3 GW

TABLE 1 Summary of the combinations considered in the study, comprising 6 WT-platform combinations, 3 turbine sizes, 7 spacing values, and 3 layout types, for a total of 378.

WT + platform [6]		Size [3]	Spacing [7]	Layout [3]
10 MW	Monopile	990 MW	5D	Radial
	Spar	1500 MW	7D	Double ring
	Semi	3000 MW	9D	Star
15 MW	Spar		11D	
	Semi		13D	
	TLP		15D	
			17D	

are selected to capture prevailing industry scales. Various internal electrical layouts and turbine spacing strategies are incorporated to characterize the trade-offs between capital expenditure and performance losses, including both wake-induced and electrical losses. For export transmission systems, multiple cable solutions are evaluated to determine their influence on energy yield and overall techno-economic performance, considering both HVAC and HVDC options typically employed for longer distances. Annual Energy Production (AEP) and Annual Hydrogen Production (AHP) are derived from long term wind resource datasets and constitute the basis for the subsequent cost assessment. The whole workflow is shown in the Figure 1.

The following sections detail the procedures adopted for techno economic analysis, together with the assumptions and datasets used to characterize wake effects, platform behaviour, and electrical losses.

2.1 Eligible area identification

The identification of suitable offshore areas represents the initial screening phase and relies on a methodology informed by Marine Spatial Planning principles. This approach ensures that only locations satisfying environmental, technical and socio-economic conditions are retained for further assessment. MSP offers a structured framework for examining offshore wind development in relation to existing maritime uses, allowing the pursuit of energy objectives while safeguarding coastal ecosystems and ensuring compatibility with marine governance. The screening procedure first excludes zones where offshore wind deployment would conflict with regulatory, ecological or operational constraints. Areas designated as Natura 2000 European Environment Agency (2025), national Marine Protected Areas and other biodiversity hotspots provided by the European Environment Agency are removed so that environmentally sensitive regions are not considered. Military and defence activity zones are eliminated using spatial layers from EMODnet (2025) to avoid interference with national security. Traffic density is incorporated and grid cells where ship movements exceed a threshold of three vessels per hour per square kilometre are discarded to prevent interaction with major shipping routes. Once these exclusion criteria are applied, technical constraints are introduced. Bathymetric data from the General Bathymetric

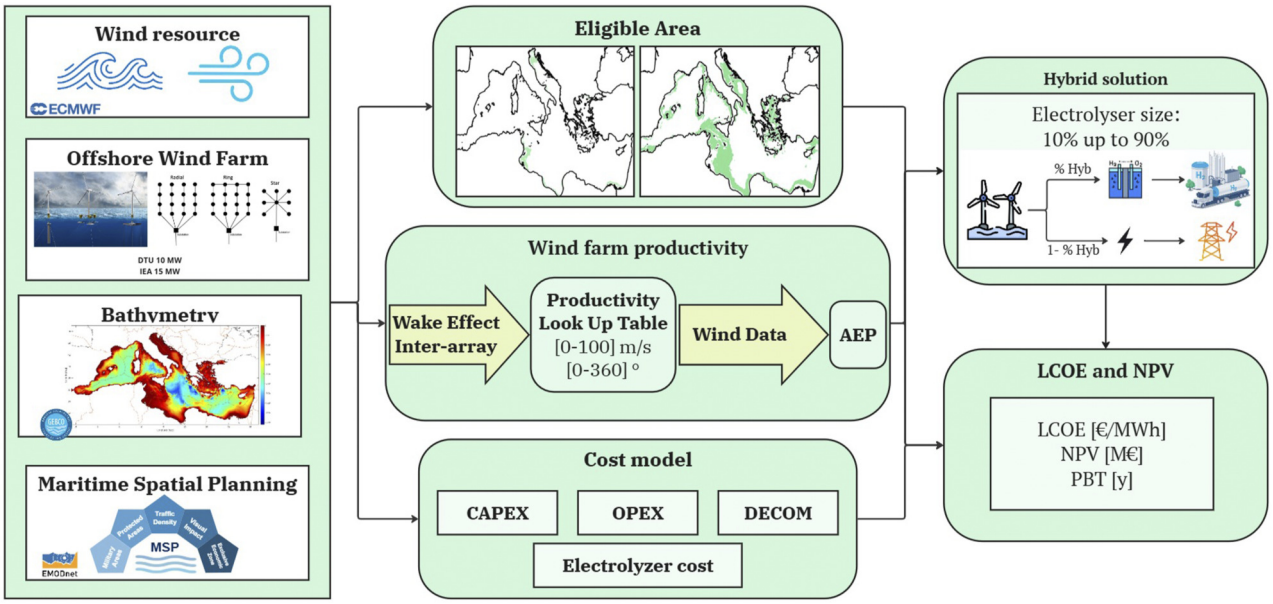

FIGURE 1
Workflow of the methodology.

Chart of the Oceans (GEBCO) GEBCO (2025) are used to define suitable depth ranges. Fixed-bottom foundations are limited to shallow waters of roughly 20–60 m Park et al. (2019), whereas floating concepts are allowed from around 60 m to approximately 1000 m, which is consistent with current technical feasibility. To reduce visual interference and limit potential conflicts with coastal activities, a minimum distance from shore of 12 km is adopted. Where relevant, proximity to existing electrical infrastructure is considered to minimise the length of export cables and enable more efficient grid connection.

TABLE 2 Wind turbine specific parameters.

Value	10 MW	15 MW	Unit
Hub height	119	150	[m]
Rotor diameter	178.3	240	[m]
Cut-in speed	4	3	[m/s]
Cut-off speed	25	25	[m/s]
Rated speed	11.4	10.59	[m/s]

2.2 Productivity methodology

The estimation of the Annual Energy Production is performed through a numerical workflow that combines high-resolution wind resource assessment with a detailed representation of turbine performance, wake interactions and electrical losses. The procedure builds on the modelling approach previously developed in Petracca et al. (2025). A preliminary database of energy yields is generated for each platform configuration. Three reference wind farm sizes are considered, namely, 0.99 GW, 1.5 GW and 3 GW, using arrays composed of 10 MW and 15 MW turbines. Four support structures are analysed: a fixed-bottom monopile configuration and three floating alternatives (spar, semisubmersible and tension leg platform). For each scenario, the wind farm is arranged according to three internal collection layouts, namely, star, radial and double ring. To assess the trade-off between wake losses and cable losses, each layout is tested with several inter-turbine spacings, ranging from 5 to 18 rotor diameters. To have a clear understanding of the amout of combninations analysed in these paper a sum up of all the combinations are provided in Table 1.

The two wind turbines selected for this study are the 10 MW DTU reference wind turbine Bak (2017) and the 15 MW IEA reference wind turbine Gaertner et al. (2020), which are widely adopted benchmark models for these power ratings. The main technical parameters of both wind turbines are reported in Table 2.

A lookup table matrix is then generated by sampling 1001 wind speed values between 0 and 100 m/s and 361 wind directions, using baseline manufacturer power curves adjusted, fist to account for performance degradation induced by Mediterranean Sea state conditions, by using the MOST tool for the hydrogynamic interaction between the platform and the sea state MOREnergyLab (2025), and then to reflect wake-induced velocity deficits, by assuming conical wake expansion model, by using the kinematic Jensen model Katic et al. (1987), and electrical losses within the wind farm following the approach presented in Faraggiana et al. (2024), by considering cable pre-sized, with a transmission level of Medium Voltage (33 kV) in alternative current. The wind resource is collected by the Copernicus European Regional Reanalysis (CERRA) dataset Copernicus Climate Change Service (C3S) (2025), which provides gridded atmospheric reanalysis data resulting from the assimilation of observations into a physical weather model. This ensures multi-year consistency and homogeneous spatial coverage suitable

for basin-scale assessments. Wind data cover a 20-year period (2001–2020), with a temporal resolution of 3 h and a spatial resolution of 0.01° × 0.01°. The original CERRA wind speeds, provided at a reference height of 100 m above sea level, are extrapolated to the turbine hub height using a logarithmic wind profile. A surface roughness length of $z_0 = 0.0002$ m, representative of offshore Mediterranean Sea conditions, is assumed. The 20 years wind time series at each grid point is then matched to the previously generated lookup tables, producing site specific AEP estimates. A turbine availability factor of 95% Elkinton (2007) is applied to account for scheduled and unscheduled downtime. Export transmission from the offshore substation to shore is modelled using either HVAC or HVDC, both operated at 220 kV. HVAC is used as baseline, while HVDC is selected for plants located in distances longer than 110 km Díaz and Guedes Soares (2023), when economically preferable. To estimate export cable length with adequate accuracy, all existing onshore substations with voltage ratings above 220 kV along the Mediterranean coastline are mapped; each offshore site is then connected to the nearest suitable substation. The annual energy production at each location is computed as:

$$AEP\left(\frac{GWh}{y}\right) = \left(\sum_{i_t}^{N_{time}} \eta_{avail} \sum_{i_T}^{N_{turb}} P_{i_T}(\theta(t), v(t)) - P_{EL}(t)\right) \frac{\Delta t}{8760} \quad (1)$$

where N_{time} the number of time steps in the selected period, $P_{i_T}(\theta(t), v(t))$ is the power output of the i_T wind turbine extracted from the interpolation with the look up table associated to wind direction, $\theta(t)$, and wind speed, $v(t)$, at time t, while $P_{EL}(t)$ is the export cable electrical losses for the cumulative power of the wind farm, and η_{avail} the turbine availability factor.

2.3 Hybrid configuration

In addition to the EtG configuration, a hybrid offshore system is examined in which the wind farm operates with both an export transmission cable (HVAC or HVDC, depending on distance, as described in Section 2.2) and a centralized offshore electrolysis plant. In this configuration, the total energy produced by the wind farm can be partitioned between direct electricity delivery to the grid and on-site hydrogen conversion SPOWIND Consortium (2025a). Hybrid systems enhance asset flexibility and potential economic performance by enabling participation in two distinct markets, electricity and hydrogen, while also providing operational redundancy: when one pathway is constrained (e.g., grid curtailment or limited hydrogen offtake), the other can temporarily absorb a larger share of the production. For hydrogen delivery to shore, two alternative transport scenarios are considered, namely, maritime transport by ship and transport via subsea pipeline. The two options are systematically compared for each offshore location, and the most cost-effective solution is selected on a site-specific basis. In general, pipeline transport is more economically attractive for sites located closer to the coast, whereas, for increasing offshore distances, hydrogen transport by ship becomes preferable due to the rapidly rising costs associated with long-distance pipeline installation. Although ship-based transport involves additional cost components, such as hydrogen liquefaction, intermediate storage, and vessel chartering, these costs become competitive at larger distances, where the required pipeline length and diameter would lead to a disproportionately higher overall investment. A detailed analysis of downstream hydrogen supply chains, including compression, liquefaction, port infrastructure, and market integration, is beyond the scope of this work and has been addressed in dedicated studies focusing on full hydrogen value-chain assessments (e.g., Farahmand et al. (2024); Sakthi and Ghahremanlou (2024)). Within the present framework, these downstream aspects are therefore treated implicitly through the adopted hydrogen price scenarios, which will be described in Section3.3. To investigate the techno-economic implications of this dual-output architecture, referring to the simultaneous production of electricity and hydrogen, the hybrid configuration is parameterized through a set of scenarios that vary the share of wind-farm output allocated to hydrogen conversion and the corresponding electrolyser size. Starting from the annual energy production previously derived, hybrid configurations are characterised by the hydrogen-dedicated capacity share f_H, defined as the fraction of the installed wind farm rated power allocated to hydrogen production. In this study, f_H is varied between 0.10 and 0.90 (10%–90%). For each scenario, the electrolyser capacity is sized accordingly, and the export cable rating is adjusted to transmit the remaining share of electricity to shore. This approach enables the identification of techno-economic trade-offs between electrolyser utilisation, cable loading, and the relative profitability of electricity and hydrogen markets SPOWIND Consortium (2025a). The main techno-economic assumptions adopted in the simulations are reported in Supplementary Table S2, while a conceptual schematic of the hybrid offshore architecture is shown in Figure 2.

With regard to the electrolyser, a proton exchange membrane electrolysers (PEMEL) are selected for offshore hydrogen production due to their ability to produce hydrogen at high pressure, operate at low temperatures, and respond rapidly to variable renewable energy inputs, which is a vital characteristic of wind energy. They also have high current density and produce high-purity hydrogen, making them efficient and compact. Additionally, PEMELs have a low environmental impact compared to other electrolyser types, although their commercial use is limited by higher costs due to expensive materials like membranes and catalysts. The power-dependent efficiency curve has been assessed using the Equation 2:

$$p = \frac{P_{ely}(t)}{P_{ely,max}}, \quad (2)$$

where p denotes the part-load ratio of the electrolyser. At full load $\eta_{el} \in [0.60, 0.65]$, with only mild efficiency loss at reduced load. For all $p \in [0.1, 0]$, the efficiency curve satisfies the condition given in Equation 3.

$$\eta_{el}(p) > 0.55 \quad (3)$$

A minimum turndown of 5%–10% capacity is allowed (PEMEL stack can idle), and the electrolyser can ramp 0%–100% output in seconds. No external power is purchased, the electrolyser only uses onsite wind farm production. The hourly power is split between the grid and the electrolyser, as shown in Equation 4.

$$P_{\text{wind}}(t) = P_{\text{grid}}(t) + P_{\text{ely}}(t). \quad (4)$$

Where $P_{\text{tot}}(t)$ is the total available wind power at hour t, $P_{\text{grid}}(t)$ is the power exported to the grid and $P_{\text{ely}}(t)$ is the power allocated

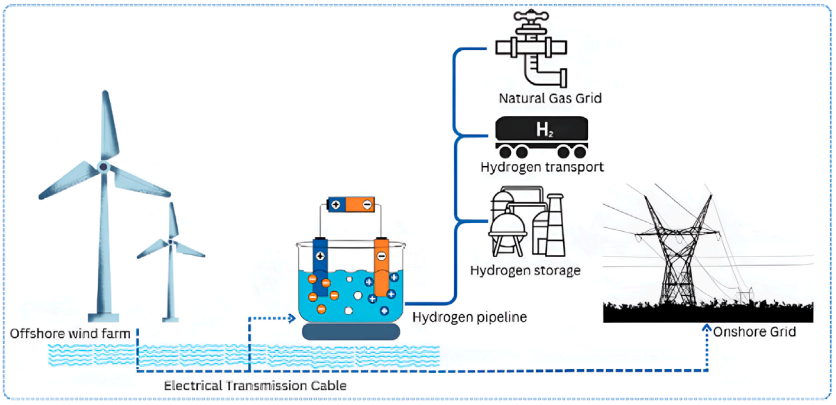

FIGURE 2
Schematic representation of a hybrid offshore wind–electrolyser system.

to electrolysis, with $0 \le P_{ely}(t) \le P_{ely,max}$, where $P_{ely,max}$ is treated as a design variable and is optimized by economic metrics. The dispatch is chosen to maximize overall value (electricity plus hydrogen revenue); in practice, an equivalent steady "split" of annual energy is used between the grid and electrolysis for the cost analysis.

As previously described in 2.2, all the wind turbines within the wind farm are gathered via inter array network to an offshore substation. Here, a portion of this power is fed into an offshore electrolyser facility; the rest (the "excess" power) is sent to shore via export cable. Further electrical losses occur in transformers and converter equipment. In the offshore-hybrid case, only minor AC-DC conversion occurs before electrolysis, since the electrolyser is located at the offshore substation.

In the offshore-centralized layout, a fraction of the wind farm's power is directed to a dedicated offshore electrolyser platform. The electrolyser is sized to capture as much energy as possible, while any surplus power is exported. Additional losses were neglected, since AC-DC conversion to power the electrolyser is assumed minimal offshore. The export cable power is then given by the remaining share of wind power, as expressed in Equation 5:

$$P_{cable}(t) = P_{farm}(t) - P_{el,off}(t), \tag{5}$$

so that only the non-utilized wind power is sent through the export cable to shore. Hydrogen production is calculated from electrolyser output. At each hour, the hydrogen mass flow rate is calculated according to Equation 6. H_2 mass rate is:

$$m_{H_2}(t) = \frac{\eta_{el} P_{ely}(t)}{LHV_{H_2}}, \tag{6}$$

where, $\dot{m}_{H_2}$ is the production rate [kg h^{-1}], η_{el} is the electrolyser efficiency at the current load fraction, P_{ely} is electrical power input to the electrolyser [kW], and LHV is the lower heating value of hydrogen, considered as 33.33 [kWh/kg]. Once the hourly hydrogen mass production rate is obtained, the corresponding AHP is computed in the same way as the AEP (Figure 1): by summing all hourly contributions and then averaging them over 1 year to determine the annual average value, expressed in [kg/y].

2.4 Techno-economic metrics

The main economic parameters to be computed for the analysis are the LCOE and NPV. LCOE represents the net present value of the quotient between the costs of operating that specific technology over the lifetime by the total amount of energy produced and it is given by the Equation 7:

$$\mathrm{LCOE} = \frac{I_0 + \sum_{y=1}^{Y} \frac{A_y}{(1+r)^y}}{\sum_{y=1}^{Y} \frac{E_y}{(1+r)^y}}, \tag{7}$$

Where I_0 represents capital investment, Y is the expected operational years (25 years), y is the current year in operation, A_y is the activity costs associated with the year y, E_y is the energy produced in year y, and r is the discount rate (8%). For the hybrid power to X case, the LCOH is defined analogously, incorporating the $CAPEX_{el}$ and $OPEX_{el}$ of the electrolyser system, and for the energy produced, it is considered the sum of annual energy production from the wind directly transmitted AEP and the equivalent energy content of the hydrogen produced ($AHP \cdot LHV$). Given the strong dependence of hybrid configurations on both electricity and hydrogen markets, a broader economic comparison, ranging from the EtG reference case to scenarios in which up to 90% of the wind-farm output is converted into hydrogen, requires the computation of the NPV under different market price assumptions. The NPV is defined in Equation 8:

$$\mathrm{NPV} = \sum_{y=1}^{T} \frac{P_{el} E_{elec}(y) + P_{H_2} m_{H_2}(y) - A_y}{(1+r)^y}, \tag{8}$$

Where P_{el} is the electricity sale price [€MWh], P_{H_2} is the hydrogen sale price [€kg] and $E_{elec}(y)$ is the electricity exported in the year y, while $m_{H_2}(y)$ is the amount of hydrogen converter in the year y. A positive NPV (above the breakeven point) indicates an economically viable investment. Within the hybrid framework, the electrolyser capacity is selected to maximize NPV, thus balancing higher hydrogen-derived revenues against the additional capital and operational expenditures. This procedure typically yields an optimal fraction of the wind farm output allocated to hydrogen conversion.

TABLE 3 Summary of CAPEX components and corresponding references.

Element	Description	References
Wind turbine	10 MW: average cost of € 10.9 M€	Energy Global (2025), Ashuri et al. (2016)
	15 MW: average cost of € 1.55 M€/MW	Catapult Offshore Renewable Energy (2023)
Platform	Fixed foundations	Ashuri et al. (2016), Catapult Offshore Renewable Energy (2023)
	Floating platforms (spar, Semi, TLP)	Díaz and Guedes Soares (2023)
Installation	Fixed foundations	Díaz and Guedes Soares (2023)
	Floating platforms (spar, Semi, TLP)	Díaz and Guedes Soares (2023)
Mooring	Cost estimated from mooring line length as a function of bathymetry	Faraggiana et al. (2024)
Electrical infrastructure	Inter-array cables and auxiliary components	Faraggiana et al. (2024)
	Export cable (see Equation 13)	Younus et al. (2025)

In addition to these three economic metrics, developers also evaluate the capacity factor of the wind farm at each site. The capacity factor represents the overall efficiency of the wind farm and is defined as the ratio between the actual annual energy production (*AEP*), previously calculated in Equation 1, and the theoretical maximum energy production that would be achieved if the wind farm operated continuously at its rated power. The latter is computed as the rated power of the wind farm, P_{rated}, multiplied by the equivalent number of hours in a year. The capacity factor is calculated according to Equation 9, following the approach proposed by Cevasco et al. (2020):

$$CF = \frac{AEP}{P_{\text{rated}} \cdot 8760}. \tag{9}$$

2.5 Cost functions

The model incorporates a full life cycle cost analysis, taking as reference the model proposed in Petracca et al. (2025), beginning with development expenditure (DEVEX), up to capital expenditure (CAPEX), decommissioning cost (DECOM) and operational expenditures (OPEX) annual cost. Starting from DEVEX, it includes site assessments, environmental studies, and licensing procedures, estimated at 142800/MW for bottom-fixed and 173918.5/MW for floating configurations Catapult Offshore Renewable Energy (2019) Catapult Offshore Renewable Energy (2023). CAPEX, computed as defined in Equation 10, encompasses the main investment cost components of the system C_{WT}, foundation construction C_{plat}, electrical infrastructure $C_{el,infr}$, installation $C_{install}$, for floating platform add also the mooring cost C_{moor}, and contingency reserves C_{cont}.

$$CAPEX = C_{WT} + C_{plat} + C_{el,infr} + C_{install} + C_{moor} + C_{cont} \tag{10}$$

Detailed information on these economic metrics is provided in SPOWIND Consortium (2025b) and Petracca et al. (2025); therefore, only a summary of the considered cost components and the corresponding references is reported here in the following Table 3.

The model accounts for economies of scale through a cost reduction factor applied to turbine and platform costs based on the number of units deployed Faraggiana et al. (2024). Regarding the PtX configurations, several cost components associated with the electrolyser system are considered. In particular, the electrolyser CAPEX includes the following elements, as detailed in Equation 11:

TABLE 4 Cost parameters of electrolysis systems, (Source: Reksten et al. (2022))

Variable	Value/Unit
k_0	673.73 €
k	10,876.9 €
α	0.662
Y_0	2020
β	−104.45
RC_0	300–600 $/kW

$$CAPEX_{\text{el}} = C_{\text{plat}} + C_{\text{el}} + C_{\text{des}} + C_{\text{conv}} + C_{\text{export}}, \tag{11}$$

where C_{plat} represents the platform cost, C_{ely} the electrolyser cost, C_{des} the desalination system cost, C_{conv} the cost of power converters, and C_{export} the hydrogen export cost. Two different hydrogen export scenarios are considered, namely, transport by ship and by pipeline, as previously described in Section 2.3. The specific electrolyser. The total CAPEX is then obtained as shown in Equation 12.

$$C_{\text{ely}} = \left[k_0 + k\, P_{\text{ely}}^{\alpha-1} \left(\frac{Y}{Y_0} \right)^{\beta} + RC_0 \right] P_{EL}, \tag{12}$$

k_0 and k are constants, P_{EL} is the rated power of the electrolyser (kWe), and Y and Y_0 are the installation year and reference year, respectively as shown in Table 4. α is a scaling exponent; typically $\alpha < 1$, indicating economies of scale (cost per unit decreases with higher power capacities), and β is a learning rate exponent; negative values ($\beta < 0$) reflect cost reductions over time due to advancements in technology and economies of scale. RC_0 is an additional fixed cost that accounts for the electrolyser-to-system costs Center on Global Energy Policy, Columbia University SIPA (2024) IRENA (2020).

The dedicated platforms required for offshore electrolysers and power substations have costs that are modeled as the expenses

related to platform equipment and platform foundations, in accordance with Singlitico et al. (2021) Danish Energy Agency (2024). The others details related to the PtX cost, in particular the different cost functions for converters, desalinator, and export in terms of ship and pipe are described in detail in SPOWIND Consortium (2025a). Then, OPEX include maintenance activities, port logistics, insurance, and monitoring systems. O&M operations can represent 20%–37% of total project costs Catapult Offshore Renewable Energy (2023) Vieira (2020) Stehly et al. (2020). The model accounts for different vessel types used in maintenance, such as Crew Transfer Vessels (CTV), Service Operational Vessels (SOV), Jack-Up Vessels (JUV) for bottom-fixed turbines, and Anchor Handling Tug Supply (AHTS) vessels for floating platforms. Insurance costs are estimated between 10,000 and 15,000 per megawatt annually, with potential reductions for farms equipped with real-time monitoring systems. Maintenance strategies are categorized into periodic and corrective operations. Periodic maintenance occurs twice per year and addresses minor failures, while corrective maintenance targets major repairs and component replacements. Failure rates for turbine subsystems are derived from industry data Carroll et al. (2015), and availability is modelled as a function of distance from port, with estimations applied for farms located more than 100 km offshore. The model uses reliability engineering principles to estimate downtime and repair frequency to simulate real-world operational variability. Abandonment Expenditures (ABEX), related to decommissioning, are calculated as a percentage of installation costs. These range from 70% to 90% for turbines and substations, and around 10% for cables Collin et al. (2017). The model also incorporates infrastructure considerations, including port upgrades and grid connection strategies. High-voltage alternating current is preferred for distances under 110 km, while high-voltage direct current is more cost-effective for longer distances. The export cable must be sized for the maximum power sent to shore. Let $P_{\max}$ denote this peak power (in MW), D the cable length to shore (km), and c the unit cost in €/MW/km. The cable capital cost is computed with the following Equation 13:

$$C_{cable} = P_{cable,max} \cdot D \cdot C_{unit}, \tag{13}$$

where $P_{\text{cable,max}}$ is the maximum cable power capacity (in MW), while D is transmission distance (km) and C_{unit} is the cost per MW per km of cable (in line with study Younus et al. (2025)). Substation costs are calculated based on transformer capacity and switchgear specifications, with offshore substations requiring significantly higher investment than onshore counterparts.

3 Results

First, the analysis reports representative outputs from the productivity and cost layers. It then presents the resulting least-cost techno-economic configurations across the eligible area.

3.1 Productivity results from lookup tables

Before presenting the techno-economic maps, the analysis reports representative outcomes from the productivity layer used in the annual energy production workflow. Farm productivity is evaluated through precomputed lookup tables that encode wake-driven efficiency as a function of inflow direction, wind speed, and turbine spacing for each wind farm layout (see Section 2.2). Figure 3 illustrates two representative cases: a ~0.99 GW farm with ~10–11 MW turbines and a 3 GW farm with 15 MW turbines. Panels (a,b) show the directional capacity factor for the densest spacing (5D, with D the rotor diameter), highlighting the strong dependence of wake losses on inflow direction and thus on the alignment between prevailing winds and the farm geometry. Panels (c,d) quantify the sensitivity of the capacity factor to turbine spacing for selected wind speeds at a fixed inflow direction: increasing spacing systematically mitigates wake-induced losses, with diminishing returns at larger separations.

These lookup-table behaviours provide the technical basis for the subsequent site-specific AEP estimation, where the 20-year wind time series is matched to the precomputed tables at each time step. In the following sections, this productivity layer is coupled with the economic cost functions to assess how layout and infrastructure choices propagate into the final techno-economic indicators, which are synthesised through the LCOE metric.

3.2 Cost drivers and economic metrics

To improve transparency on the main economic drivers, the analysis first reports how key cost components vary with the dominant spatial variables in the Mediterranean: distance to shore and bathymetry. Figure 4 summarizes the cost trends used in the economic analysis across the full design space.

Distance to shore primarily affects installation logistics, export infrastructure, and OPEX. Installation-related costs increase with distance due to longer vessel transit times and extended weather windows, with different cost trajectories observed for bottom-fixed foundations and among the different floating substructures. Export cable costs scale with both distance and cable rating; therefore, larger wind-farm sizes and higher export capacities lead to higher infrastructure costs for the same offshore distance. The export cable cost profiles also reflect the adopted transmission technology: as described in Section 2.5, HVAC solutions are selected for distances below 110 km, while HVDC transmission is adopted beyond this threshold, resulting in a distinct cost behaviour in the reported results. In addition, OPEX increases with distance, as maintenance and corrective interventions require longer mobilisation times and higher vessel day rates. Bathymetry mainly affects floating systems through mooring requirements. As water depth increases, mooring line length and associated hardware requirements rise, leading to higher mooring CAPEX and influencing the relative cost competitiveness among the floating platforms considered. Among the analysed concepts, the TLP exhibits the lowest mooring costs and the weakest sensitivity to water depth, while spar and semisubmersible platforms show a stronger dependence on bathymetry. For hydrogen export, Figure 5 compares the two delivery options considered, pipeline and ship, as a function of distance. The figure reports results for the optimal PtX configuration, showing both the median trend and the distribution across all spatial points. The observed cost patterns are not perfectly linear with distance, as hydrogen export costs are also influenced by site-specific productivity and the wind-farm capacity factor. Consistent with Section 2.3, pipeline export

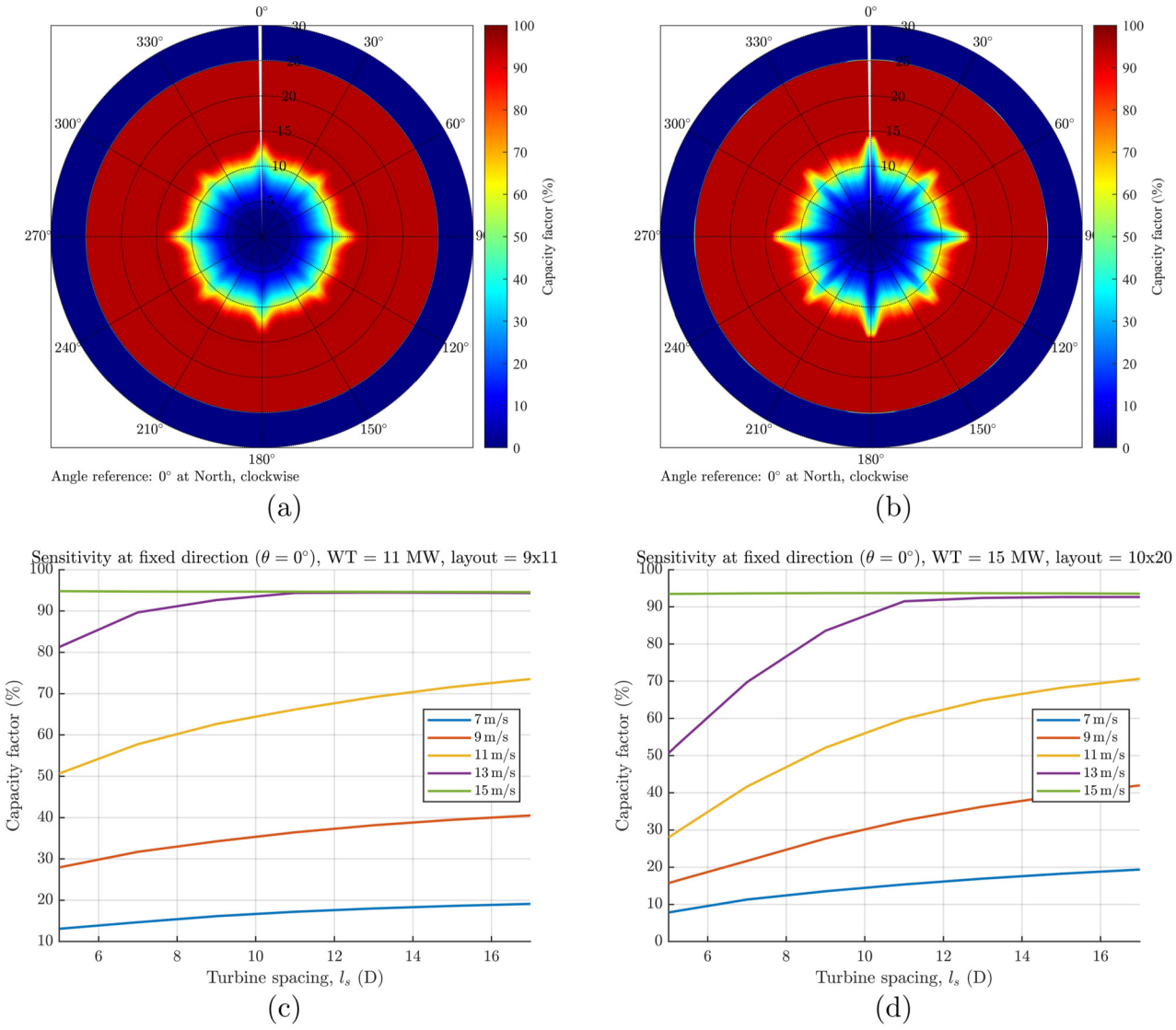

FIGURE 3
Examples of productivity look-up tables. Directional capacity factor at 5*D* spacing for the ~0.99 GW farm **(a)** and the 3 GW farm **(b)**. Capacity-factor sensitivity to turbine spacing for selected wind speeds at a fixed inflow direction for the ~0.99 GW farm **(c)** and the 3 GW farm **(d)**.

is generally more attractive at shorter distances, whereas ship-based transport becomes preferable as distance increases due to the rapidly rising installation costs of long pipelines. These trends are subsequently reflected in the hybrid LCOH and investment metrics.

3.3 Techno-economic results and optimal configurations

Building on the productivity and cost drivers discussed above, the following results summarise the resulting optimal techno-economic configurations across the investigated sites, where optimality is defined as the minimum LCOE obtained at each spatial location among the 378 analysed combinations (Table 1) of wind turbine rating, support structure, wind farm size, layout, and spacing. The results indicate that the radial internal layout provides the most advantageous trade-off between spatial extent and electrical losses. This configuration minimizes cable related expenditure while maintaining high energy yield. In contrast, star and double-ring arrangements exhibit both higher costs and higher electrical losses, although they inherently offer greater redundancy. Since the present study focuses exclusively on techno-economic performance, the configuration selected as optimal is the one achieving the best balance between cost and losses, without explicitly valuing redundancy. Optimal turbine spacing is similarly determined by balancing wake-induced losses against electrical losses within the internal grid. The resulting optimal spacing for each analysed point is shown in Figure 6. These optimal distances are predominantly associated with larger wind farms; consequently, under the cost assumptions adopted in this study, the resulting values tend to be higher, reaching mainly spacing distances of around 15 rotor diameters. This indicates that wake losses exert

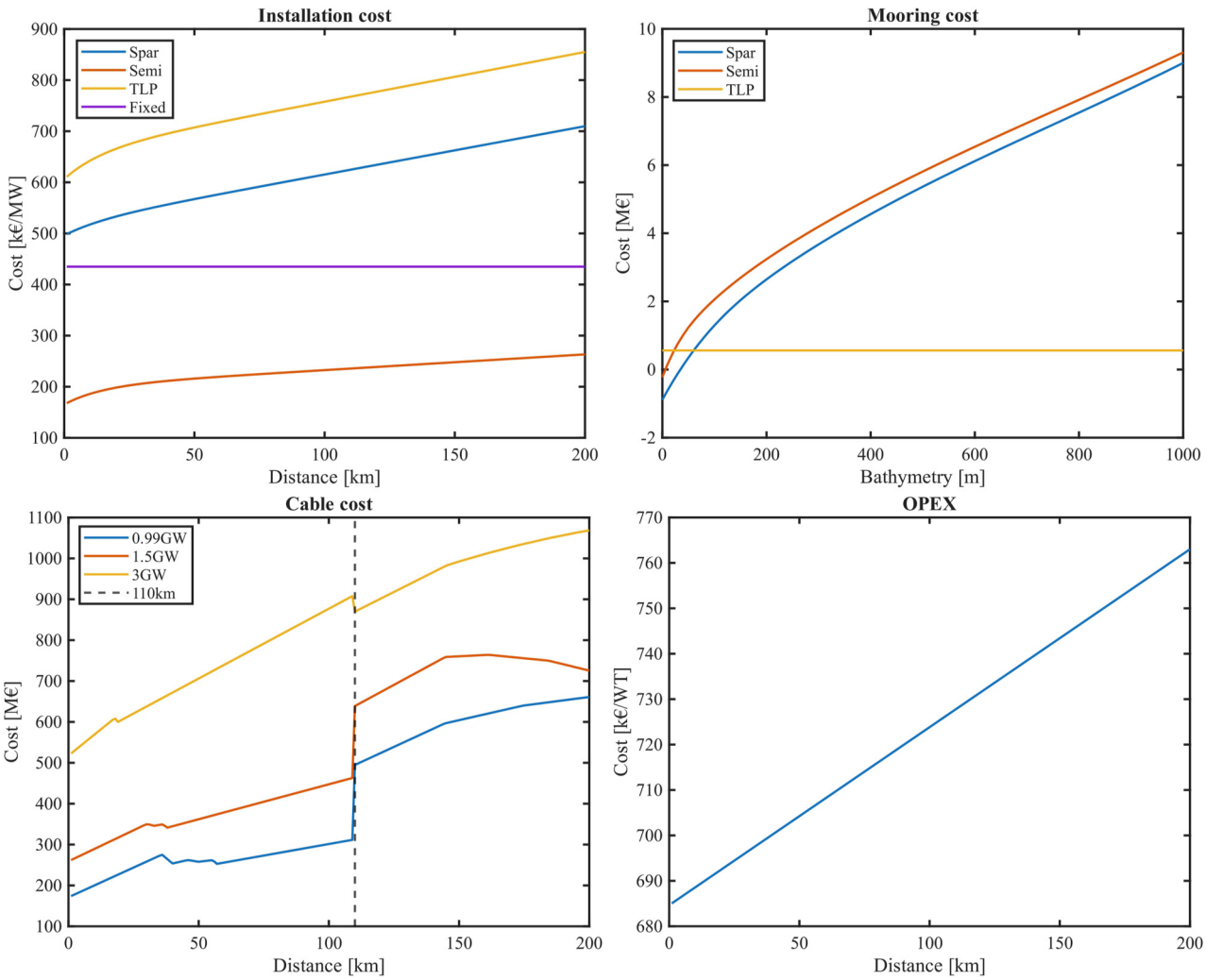

FIGURE 4
Results of economic metrics as function of main combination considered and distance or bethymetry.

a stronger influence on the optimal layout than cable costs or electrical losses.

With regard to farm size and support structure, the analysis shows that fixed-bottom sites are economically optimal for a 1.5 GW wind farm, whereas floating sites perform best at smaller capacities, particularly the 990 MW configuration using 15 MW turbines. In particular, to better illustrate how fixed and floating wind farms are distributed within the overall eligible area, the specific eligible zones for fixed and floating installations are outlined in Figure 7.

In order to perform the further analysis with the configuration associated with the best performance, the hybrid cases were subsequently performed using the full wind baseline simulations and their corresponding optimal configurations as reference, which consist, to sum up, on the radial layout applied to a 1.5 GW fixed-bottom wind farm equipped with 10 MW turbines, and to a 0.99 GW floating wind farm equipped with 15 MW turbines, with the spacing shown on Figure 6. The same assessment procedure is applied to all hybrid scenarios, each defined by a different share of wind farm energy allocated to hydrogen production, as previously described in Section 2.3. However, as shown in Figure 8, the optimal hybrid configurations cannot be directly compared with the full wind case (Figure 6) given the fundamentally different cost and efficiency structures. In particular, the minimum LCOE achieved in the hybrid configuration is 81.4€/MWh, whereas the full wind farm case reaches a substantially lower value of 48.37€/MWh.

Therefore, as might be expected, the configuration selected as optimal in the hybrid scenario is always the one with the lowest f_H, namely, the 10% conversion case, Figure 8 (right). This indicates that, under current cost assumptions, increasing the f_H consistently worsens the techno-economic performance, and the economic optimum remains as close as possible to the EtG configuration. Hence, in order to obtain a more comprehensive and consistent economic evaluation, a sensitivity analysis is subsequently performed using the NPV and PBT as key indicators. This analysis explores a range of electricity and hydrogen price scenarios, thus providing a broader view of the conditions under which hybrid systems can become economically competitive. The selected price ranges are grounded in current market benchmarks: hydrogen

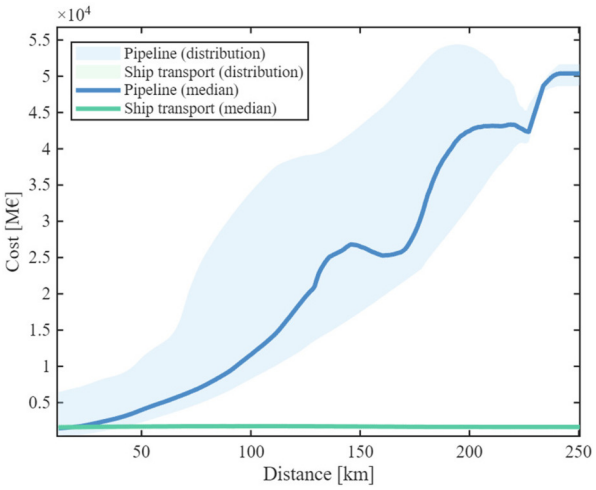

FIGURE 5
Results of PtX transport economic metrics (CAPEX + OPEX) for the two scenarios considered (ship and pipeline) as function of the distance.

prices follow projections for green hydrogen (Younus et al. (2025); Hill et al. (2024)), while electricity prices are derived from the day-ahead market GME Mercato Elettrico (2025). These reference prices for hydrogen and electricity constitute the baseline from which the average values are defined. The resulting average prices are 9€/kg for hydrogen and 110€/MWh for electricity. To ensure a uniform distribution across the price ranges and scenarios, variations of ±20% and ±40% are then applied to the baseline, enabling a broad exploration of possible market conditions, obtaining a set of 25 combinations. Thus, the electricity prices are 65, 90, 110, 130, 155€/MWh and the hydrogen prices are 5.5, 7, 9, 11, 12.5€/kg. From the set of combinations analysed, three representative price scenarios were analysed for the preliminary presentation of results. The "mid-range" scenario adopts the mean hydrogen and electricity prices (9€/kg and 110€/MWh); the "hydrogen-convenient" scenario combines higher hydrogen prices with lower electricity prices (12.5€kg and 65€/MWh); and the "electricity-convenient" scenario assumes the opposite condition, with higher electricity prices and lower hydrogen prices (5.5€/kg and 155€/MWh).

In the following maps, the spatial distribution of the 25-year NPV is shown for all three market scenarios, displaying only the locations where the NPV is positive, thus highlighting the areas for which offshore development is economically viable. At each point, the result shown corresponds to the configuration that yields the highest NPV among all those evaluated. It is worth noting that the spatial extent of economically viable locations varies substantially across scenarios: 62.15% of the eligible area achieves NPV $>$ 0 in the mid-range case, increasing to 92.9% under electricity-convenient conditions, while it drops to 32.8% in the hydrogen-convenient scenario. Across the evaluated price scenarios, the techno-economic performance of the EtG and hybrid configurations exhibits distinct patterns driven by the relative values of electricity and hydrogen. Under the reference case, Figure 10, characterized by "mid-range" prices for both commodities, the results show that the EtG configuration generally remains the most economically favorable option. In this scenario, the additional conversion losses and the higher capital requirements associated with offshore electrolysis are not compensated by hydrogen revenues, making direct electricity export the preferable pathway. The inclusion of the boxplot in Figure 10 highlights the variability of NPV across all viable sites. While maximum NPV values reach about 3,764 M, the median is significantly lower (approximately 580 M), indicating that only a limited subset of locations concentrates the highest profitability. Consistent with this observation, only 62.15% of the domain remains economically viable, reflecting that moderate electricity prices limit achievable revenues even where the EtG configuration is selected as optimal. These results are comparable with other findings in the literature D'Adamo et al. (2025), which report a cost range from 0.195 up to 1.3 M/kW, consistent with the distribution observed in our analysis.

A markedly different trend appears under the "hydrogen-convenient" scenario, Figures 9, 10, defined by high hydrogen sale prices and comparatively low electricity prices. In this case, hybrid configurations become consistently more attractive, and the optimal solutions shift towards higher f_H. The corresponding boxplot in Figure 10 shows that maximum NPVs increase to around 4,069.7 M, while the median rises to 789 M, noticeably higher than in the reference scenario. These results confirm that hydrogen-favorable market conditions enhance profitability for many sites, although such conditions do not uniformly translate into economic viability. After applying the positive-NPV filter, only 32.8% of the area remains viable, meaning that many points where hybrid configurations appear technically optimal do not achieve sufficient revenues to offset the higher capital expenditure. The favorable locations therefore cluster around areas where high f_H can fully take advantage of the elevated hydrogen price, while all areas associated with the EtG configurations are filtered out, Figure 9.

Conversely, in the "electricity-convenient" scenario, Figure 10, characterized by elevated electricity prices and low hydrogen prices, the EtG configuration is always selected. The boxplot associated with this scenario shows a marked upward shift in profitability, with maximum NPVs reaching around 7,149.3 Mand a median of 1,696 M, the highest among all evaluated cases. Under these electricity-driven market conditions, nearly the entire set of technically eligible locations (92.9%) achieves a positive NPV, making the economic filter far less restrictive. As a consequence, the resulting map retains almost all viable sites, confirming that high electricity prices strongly favor conventional offshore wind over hybrid alternatives. To further investigate the factors driving the selection of hybrid configurations across the Mediterranean sea, an additional sensitivity analysis was performed by relating the optimal f_H to the local wind resource. This analysis focuses on the hydrogen-convenient scenario, which provides the widest range of economically viable hybrid outcomes. The results, shown in Figure 11, reveal a clear correlation between wind speed and the f_H. The correlation is assessed with respect to the wind resource rather than the resulting productivity, in order to avoid introducing dependencies on the chosen configuration itself, which could otherwise bias the interpretation of the results. As a result, areas characterised by moderate wind resources tend to select either EtG (0%) or low-conversion configurations, whereas higher wind speeds progressively favour larger f_H. This trend reflects the underlying economic behaviour of the system: locations with stronger wind conditions, and thus higher productivity,

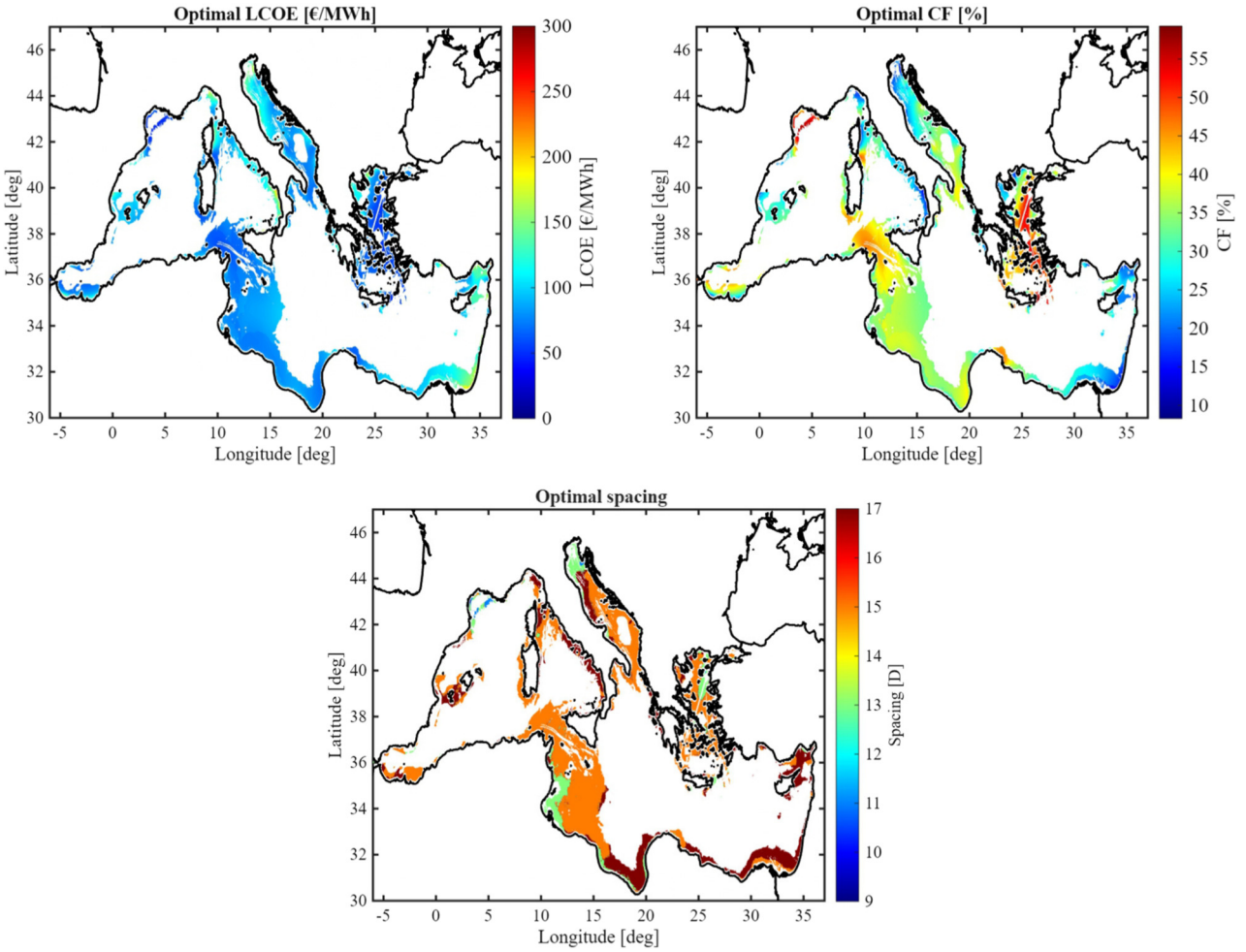

FIGURE 6
Optimal results for full wind configuration: LCOE, CF and spacing.

can more easily sustain the additional capital expenditure and efficiency penalties associated with hydrogen production, whereas low-resource sites cannot compensate for these costs through increased energy yield. Moreover, because electrolyser efficiency decreases under reduced-load operation, oversizing the unit, and so higher f_H, leads to operate at lower power fractions and therefore to reduced hydrogen conversion efficiency. Therefore, areas characterised by low wind resource (i.e 5 m/s) typically results in an f_H of 0.1, or even 0.

The Figure 11 therefore complements the previous spatial analysis by illustrating that the emergence of hybrid configurations is not driven only by market assumptions but is also strongly conditioned by local productivity. Together, these results show that hybridisation becomes attractive only where both favourable market signals and sufficiently high wind resources coexist, thereby explaining the spatial patterns observed in the hydrogen-convenient maps Figure 8 and the dominance of EtG configurations in the electricity-convenient scenario in Figure 10. To complement the previous analyses and provide an overall view of how often each configuration emerges as economically favourable, Figure 12 summarizes the aggregated results across all market scenarios considered, showing the relative frequency with which each conversion level is selected as optimal. The bars represent the share of occurrences associated with each f_H (from 10% to 90%), together with the electrical-to-grid baseline case. As also highlighted by the dominant presence of the EtG category across most scenarios, direct electricity export generally remains the most favourable option under current market conditions. When hybridisation becomes competitive, the most frequently selected configuration within the hydrogen-convenient scenario corresponds to a f_H = 50%, indicating that mid-range split configurations maximise the overall economic performance under favourable hydrogen-price conditions. However, when considering all scenarios collectively, the optimal hybrid configurations tend to shift toward lower f_H, with the 20% and 30% cases occurring most frequently overall. This suggests that, outside hydrogen-advantageous market conditions, lower f_H offer a more robust balance between electrolyser utilisation, cable loading, and the relative value of electricity and hydrogen revenues.

The Figure 12 also highlights, across all market scenarios analysed, the conditions under which hybrid configurations outperform the EtG alternative, even if only in a subset of locations. Starting from 130/MWh, only a small share of PtX solutions appears.

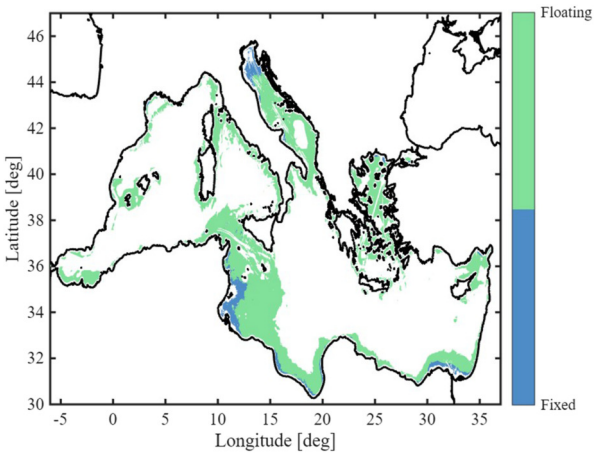

FIGURE 7
Eligible area for floating (blue) and fixed (green) wind farm installations.

As the electricity price decreases towards 65/MWh, and hydrogen remains at the high end of the assumed range, the occurrence of PtX configurations increases markedly, reaching about 96.7% of the eligible area in the hydrogen-convenient scenario, with a relatively homogeneous distribution of f_H.

3.4 Case study sensitivity (NPV and PBT)

Based on the optimal configurations identified in the previous sections, the detailed evolution of the NPV over the 25-year operational lifetime is examined, together with the corresponding PBT. The analysis shift towards a specific case study site (located in the Gulf of Lyon), with the highest NPV. This site is firstly evaluated for the EtG configuration under varying electricity-price conditions (Figure 13A), and subsequently for the hybrid configuration, specifically for f_H = 50%, which was previously identified as the optimal most selected in the hydrogen-convenient scenario.

The hybrid case is assessed under two complementary perspectives: by fixing the hydrogen price at the most favorable value and varying electricity prices, and by fixing the electricity price at a representative mid-range level while varying hydrogen prices. The resulting NPV trajectories show that the EtG configuration exhibits a strong dependence on electricity-market conditions, Figure 13B. When electricity prices exceed approximately 90€/MWh, the project reaches a positive NPV within the first decade, with profitability increasing significantly at higher prices. The best results, corresponding to the higher electricity price scenario (155€/MWh), show a payback time of 4 years. This outcome is significantly lower than values reported in the current state of the art D'Adamo et al. (2025), which is typically around 1 decade; however, it should be noted that the analysis refers to the most favorable economic scenario and to the location characterized by the highest techno-economic performance. Therefore, as highlighted by the wide distribution shown in the map in Figure 10, a broader spread of values toward higher PBT can be expected. In contrast, the hybrid configuration displays a more moderate response to electricity-price variation (Figure 13B), but a pronounced sensitivity to hydrogen prices. Under favourable hydrogen-price conditions (11–12.5/kg), the 50% hybrid system attains NPV values comparable to those of the EtG case (Figure 13A). In these cases, the hybrid configuration achieves acceptable NPV values, with payback times of approximately 13–15 years, although still not comparable to the EtG solution, which reaches NPV = 0, after about 6 years in the same electricity price condition. A distinctive feature emerging in the hybrid case is the presence of two local decreases in the NPV curves, occurring around years 9 and 18. These reductions, which do not appear in the EtG trajectories, are a direct consequence of the electrolyser replacement events included in the economic model. The associated reinvestment costs temporarily offset cumulative revenues, causing the NPV to decline before resuming its upward trend. Finally, when hydrogen prices fall below approximately 5.5–7/kg, the hybrid configuration remains unprofitable over the entire project lifetime, regardless of electricity-price assumptions, confirming that market conditions play a decisive role in determining the economic viability of offshore wind-hydrogen systems. Taken together, these trends indicate that hybrid offshore wind-hydrogen systems become economically competitive only under hydrogen-driven market conditions, where revenue from hydrogen sales compensates for conversion losses and higher capital costs. Conversely, when electricity prices dominate market value, the EtG configuration consistently yields superior economic performance. The analysis of NPV evolution thus reinforces the conclusions drawn from the occurrence-based selection, providing a coherent and comprehensive understanding of the circumstances under which hybridization can represent a viable alternative to conventional wind-to-grid solutions.

4 Conclusion and discussion

This study presents a detailed techno-economic evaluation of offshore wind development in the Mediterranean Sea, with particular attention to hybrid wind-to-hydrogen configurations. The work responds to a gap in literature, where the optimal sizing of offshore electrolysers and the conditions under which hybrid systems may become advantageous have not been investigated in a spatially explicit way. By combining site eligibility screening with wind farm modelling and a multi-scenario economic analysis, the methodology proposed here allows the identification of the most suitable configuration for each location and provides a coherent basis for comparison between different hybrid layouts. To support the interpretation of the spatial techno-economic results, the analysis explicitly separates the technical productivity layer, represented through lookup tables capturing wake and layout effects, from the main economic cost drivers. This layered approach allows the optimal configurations to be interpreted as the outcome of well-defined physical and economic mechanisms, rather than as purely numerical optimisation results. The results show that, with current costs and efficiencies, direct electricity export remains the most competitive option across the Mediterranean. This is particularly evident under market conditions resembling the "mid-range" scenario, represented in this study by electricity prices of around 110/MWh and hydrogen prices of 9/kg. Under these conditions, all suitable sites achieve a positive NPV and are characterized

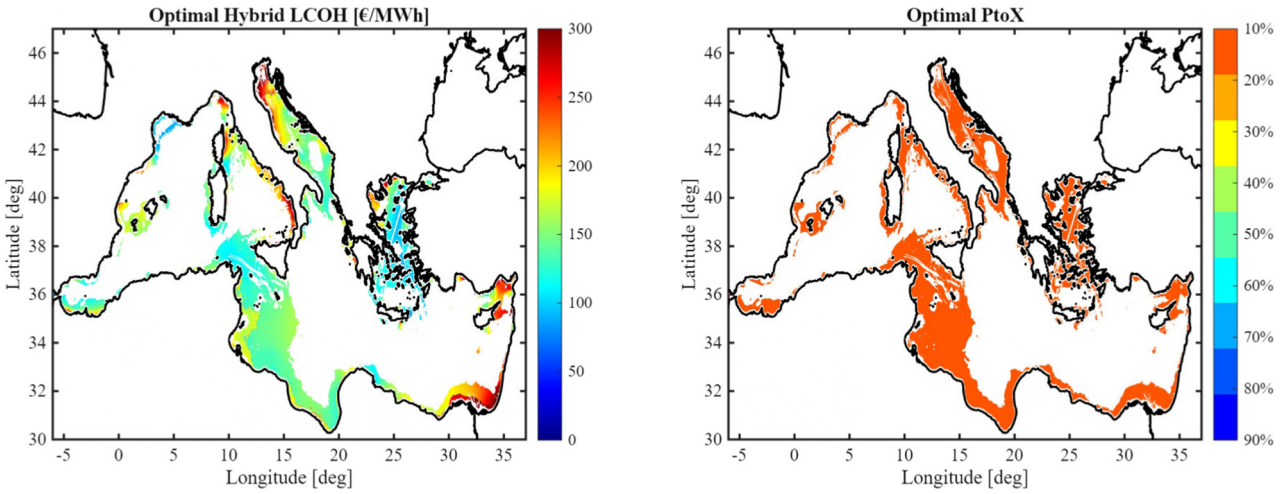

FIGURE 8
Optimal levelized cost of hydrogen in equivalent energy content/MWh (left) and optimal configuration chosen (right).

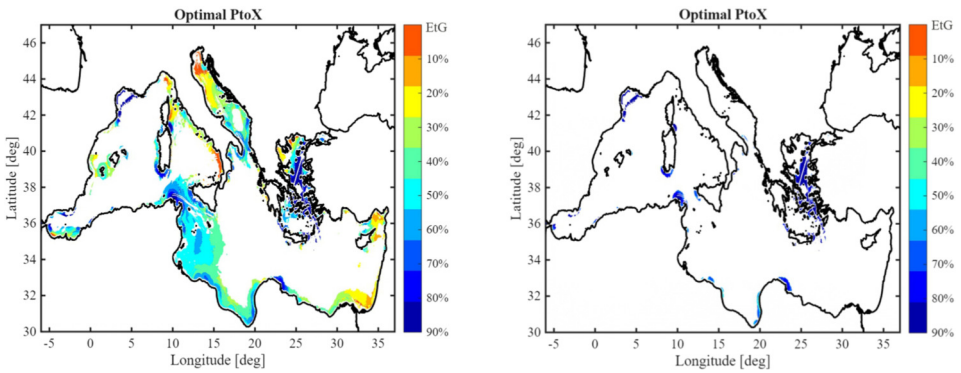

FIGURE 9
Optimal configurations for the "hydrogen-convenient" price scenario (65/MWh, 12.5/kg), shown for the entire study area (left) and for the economically advantageous subset (right).

by the baseline EtG configuration. No incentives or subsidies are included in the analysis, so these outcomes reflect exclusively market-driven conditions. Hybrid configurations generally perform worse in the baseline scenarios because of higher investment requirements and losses associated with the conversion to hydrogen. This behaviour is also confirmed by the internal comparison among hybrid options, where the f_H = 10% conversion case is consistently selected as the most convenient (Figure 8). Increasing f_H systematically reduces economic performance under the present cost assumptions. However, the results also show that hybrid systems can become competitive when the hydrogen market is sufficiently favourable. In fact, in the "hydrogen-convenient" scenario used in this work, defined by relatively low electricity prices and hydrogen prices in the range of 12.5/kg, several hybrid configurations reach NPVs comparable and higher than those of EtG systems. In this context, intermediate conversion levels, particularly f_H = 50% case, emerge as the most promising solutions. A clear dependence on the local wind resource is also observed since only the areas with the highest wind speeds are able to sustain the additional costs associated with electrolysis (Figure 11). The occurrence-based analysis across all market combinations, reported in Figure 12 reinforces these findings. Hence, hybrid configurations become attractive only under favourable hydrogen-price conditions, where intermediate f_H tend to perform best. Across all market scenarios, however, lower f_H emerge more consistently as robust solutions, offering a balanced trade-off between asset utilisation and revenue streams. Finally, the NPV trajectories reinforce the main economic patterns observed in the occurrence-based analysis. EtG baseline configurations generally achieve positive NPV within the first decade, whereas hybrid systems progress more slowly and remain more exposed to hydrogen-market conditions. The temporary NPV declines appearing in hybrid trajectories, caused by scheduled electrolyser replacements, highlight the role of reinvestment cycles in shaping long-term profitability. Under unfavourable hydrogen prices (below approximately 5.5–7/kg), hybrid systems do not reach profitability over the project lifetime, independent

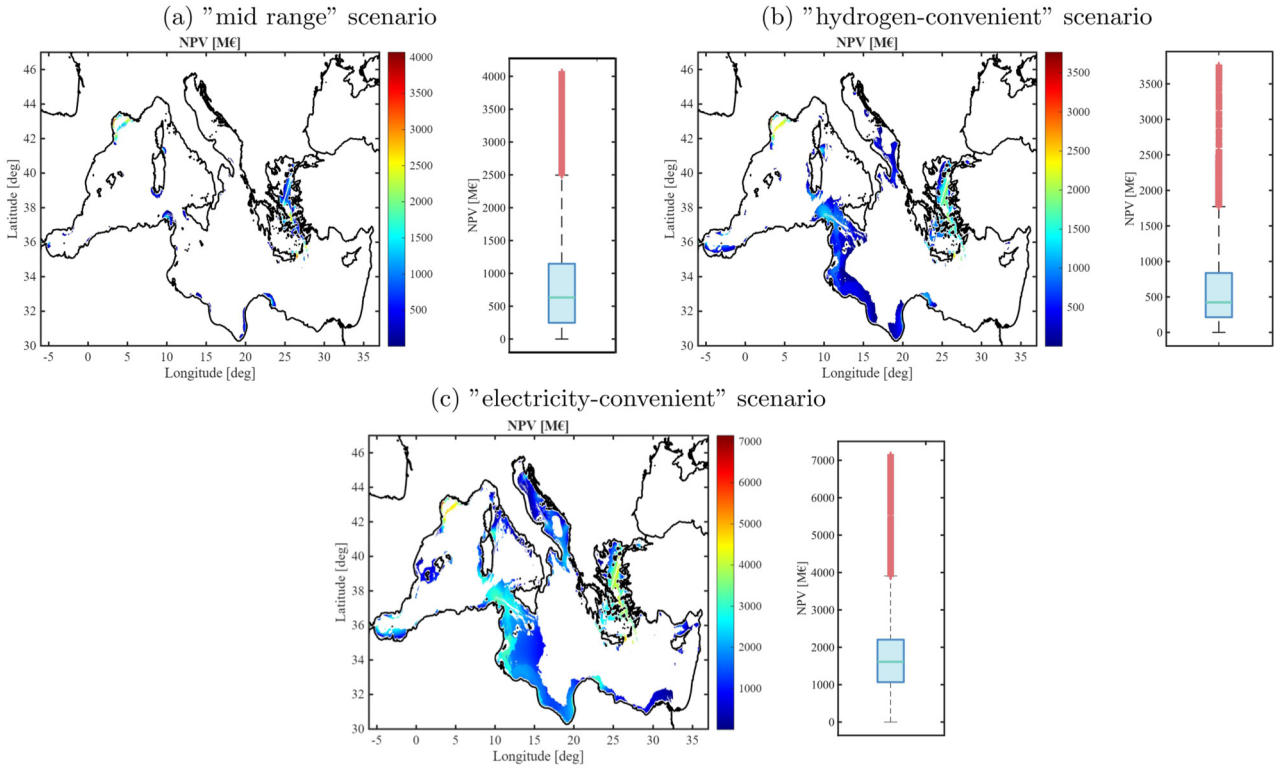

FIGURE 10
NPV spatially distribution across all eligible locations for the three market scenario: **(a)** "mid-range", **(b)** "hydrogen-convenient", **(c)** "electricity-convenient".

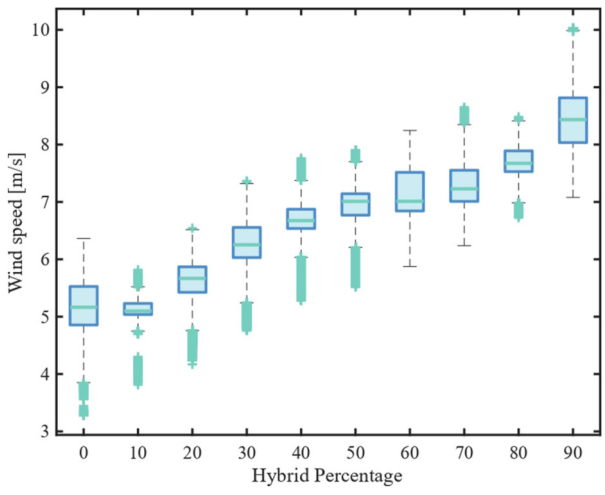

FIGURE 11
Hybrid optimal percentage selection based on wind speed, for "hydrogen-convenient" scenario.

of electricity-price assumptions. Overall, these results confirm that hybrid offshore wind-to-hydrogen systems become economically competitive only under hydrogen-advantageous market conditions, whereas EtG solutions retain superior performance across a wider range of market scenarios, particularly when electricity value dominates. In the current Mediterranean context, hybridisation is therefore not yet the most cost-effective option, although improving hydrogen markets and evolving cost structures may shift this balance in the coming years. However, this conclusion should be interpreted according to the intrinsic limitations induced by the cost-based metrics adopted in this work. Coherently with what has already been mentioned in the introductory section, hybrid offshore wind–hydrogen systems provide additional value streams with respect to those expressed using electricity-equivalent terms. The possibility of converting excess generation into chemical energy, instead of curtailing it, is only one example of power-to-X benefits. In addition, grid deferral value, namely, the economic saving generated by mitigation of transmission bottlenecks and the reduction of peak power injections, as well as export optionality explore the potential of hydrogen as a storable, tradable, and exportable energy vector. Additional content concerning this discussion may be found in Borsboom-Hanson et al. (2022). Moreover, offshore wind–hydrogen integration can be examined from the perspective of energy security and diversification. These features allow hybrid systems to be regarded not merely as alternatives to grid connection, but also as strategic infrastructure supporting long-term decarbonization and energy independence. Moreover, the proposed workflow is readily transferable to other emerging offshore wind–hydrogen regions (e.g., Atlantic Canada, the Western U.S., and offshore hydrogen hubs Borsboom-Hanson et al. (2022)), as it relies on modular inputs, spatial constraints, long-term wind fields,

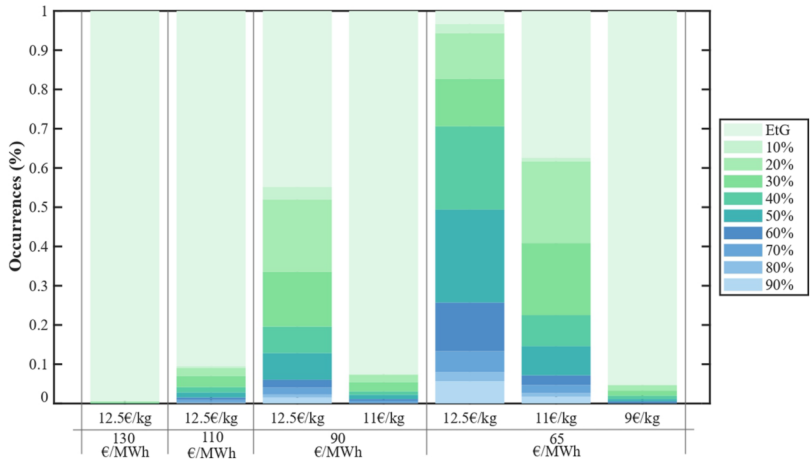

FIGURE 12
Comparison between all hybrid configurations and full wind farm, in different market scenarios.

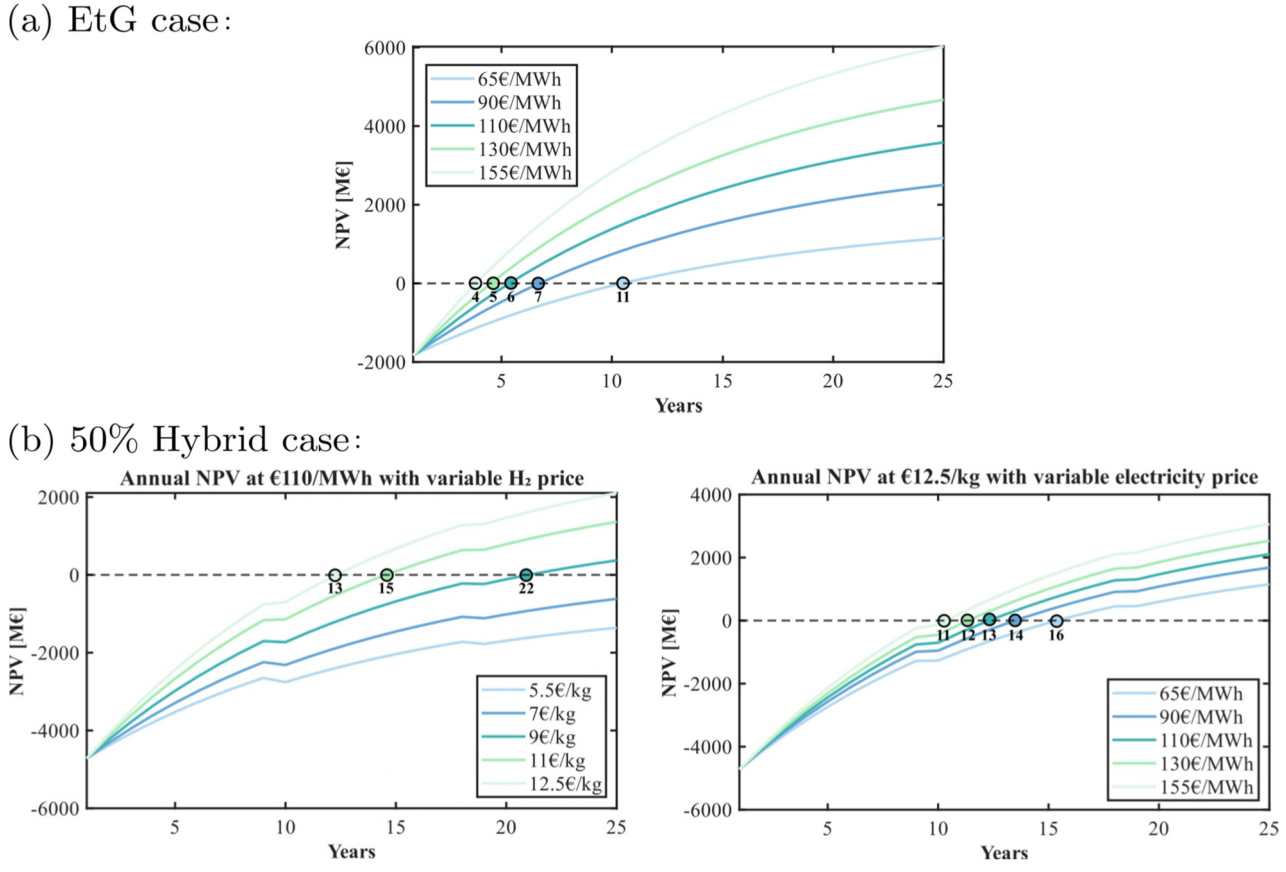

FIGURE 13
NPV and PBT associated to the best point in terms of higher NPV for **(a)** EtG and **(b)** f_H = 50%.

bathymetry, and distance-to-infrastructure cost functions, that can be re-parameterised with local datasets and permitting rules.

The methodology developed in this study offers a transparent framework for evaluating these trade-offs and for identifying conditions under which hybrid configurations could become attractive. While the analysis provides meaningful insights into the relative performance of the two configurations, several limitations should be acknowledged. First, the results are strongly influenced

by the cost models adopted for offshore wind technologies and electrolysers, including assumptions on CAPEX, efficiencies, lifetimes, and replacement cycles. Although based on the best available techno-economic data, these parameters carry significant uncertainty, and deviations in future cost or performance trends could markedly affect the comparative competitiveness of hybrid systems. A second limitation concerns the representation of hydrogen prices, which strongly influences the profitability of hybrid systems. Although a broad price range is explored to reflect different possible market conditions, the analysis is performed without considering incentives, subsidies, or regulatory support. This allows for an assessment under purely market-driven dynamics but does not capture the policy framework likely to accompany the deployment of offshore wind and green hydrogen. Mechanisms such as contracts for difference, targeted electrolyser support, or preferential grid access could substantially modify the relative performance of the configurations assessed. A further limitation concerns the exclusive focus on economic performance, evaluated only through hydrogen sales. The analysis does not account for ancillary benefits that hybrid configurations may offer, such as enhanced system resilience, improved integration of variable renewable energy, or the ability of electrolysers to smooth production fluctuations and reduce curtailment. These operational advantages could generate additional value under real-world conditions but lie outside the scope of the present modelling framework. A complementary next step is to couple the spatial cost maps with explicit policy scenarios (e.g., carbon-price trajectories, support schemes and congestion constraints), enabling a quantitative mapping between policy instruments and viability thresholds for offshore wind-to-hydrogen investments. To achieve a more comprehensive assessment of the economic feasibility of hydrogen and, more generally, of the potential advantages of hybrid PtX configurations, future work should incorporate policy scenarios, operational flexibility, system-integration benefits, and environmental considerations. Such an expanded approach would provide a clearer understanding of the conditions under which offshore wind-to-hydrogen hybrid systems may become advantageous in the Mediterranean context.

Data availability statement

The author(s) declared that financial support was received for this work and/or its publication. This work was funded by the SPOWIND project (Euro-MED0200199), financed by the Interreg Euro-MED Programme under the Smarter MED priority, which also covered the article processing charges.

Author contributions

VD: Software, Methodology, Writing – review and editing, Investigation, Supervision, Conceptualization, Writing – original draft, Resources, Visualization, Data curation, Formal Analysis, Validation. EP: Supervision, Data curation, Software, Formal Analysis, Methodology, Visualization, Resources, Conceptualization, Validation, Investigation, Writing – review and editing, Writing – original draft. FJ: Methodology, Data curation, Resources, Formal Analysis, Writing – original draft. AB: Formal Analysis, Resources, Data curation, Methodology, Writing – original draft. GMn: Data curation, Formal Analysis, Resources, Writing – review and editing, Methodology. CN: Data curation, Resources, Writing – review and editing. GR: Writing – review and editing. JM: Resources, Writing – review and editing, Formal Analysis, Data curation, Methodology. AD: Writing – review and editing, Supervision. DnG: Formal Analysis, Supervision, Writing – review and editing. DvG: Project administration, Writing – review and editing, Supervision. GMg: Writing – review and editing, Supervision. EG-P: Writing – review and editing, Supervision, Formal Analysis, Resources, Writing – original draft, Methodology. GB: Writing – review and editing, Funding acquisition, Project administration, Supervision.

Funding

The author(s) declared that financial support was received for this work and/or its publication. This work was funded by the SPOWIND project (Euro-MED0200199), financed by the Interreg Euro-MED Programme under the Smarter MED priority, which also covered the article processing charges.

Acknowledgements

This work was developed within the SPOWIND project (Euro-MED0200199), funded by the Interreg Euro-MED Programme under the Smarter MED priority. The project is coordinated by Politecnico di Torino in collaboration with international partners. We acknowledge the support of all consortium members and stakeholders contributing to the development of marine spatial planning tools for offshore wind energy in the Mediterranean. The authors express their gratitude for the funds received from the Ministry of University and Research and PNRR's PhD scholarship program defined in DM-352/2022 in collaboration with Eni S. p.A. This publication is part of the PNRR-NGEU project.

Conflict of interest

Author GR was employed by ENVPRO.

Author JM was employed by EDP NEW.

The remaining author(s) declared that this work was conducted in the absence of any commercial or financial relationships that could be construed as a potential conflict of interest.

Generative AI statement

The author(s) declared that generative AI was not used in the creation of this manuscript.

Any alternative text (alt text) provided alongside figures in this article has been generated by Frontiers with the support of artificial intelligence and reasonable efforts have been made to ensure accuracy, including review by the authors wherever possible. If you identify any issues, please contact us.

Publisher's note

All claims expressed in this article are solely those of the authors and do not necessarily represent those of their affiliated organizations, or those of the publisher, the editors and the reviewers. Any product that may be evaluated in this article, or claim that may be made by its manufacturer, is not guaranteed or endorsed by the publisher.

Supplementary material

The Supplementary Material for this article can be found online at: https://www.frontiersin.org/articles/10.3389/fenrg.2026.1765111/full#supplementary-material

References

AquaDuctus Offshore/GASCADE Gastransport GmbH (2026). Aquaductus: hydrogen infrastructure in the north sea. Available online at: https://aquaductus-offshore.de/ (Accessed January 30, 2026).

Ashuri, T., Zaaijer, M. B., Martins, J. R. R. A., and Zhang, J. (2016). Multidisciplinary design optimization of large wind Turbines—technical, economic, and design challenges. *Energy Convers. Manag.* 123, 56–70. doi:10.1016/j.enconman.2016.06.004

Avesani, M. (2025). The mediterranean offshore wind turn: lessons, risks, and regional reflections [version 3; peer review: 1 approved, 2 approved with reservations]. *Open Res. Eur.* 5, 66. doi:10.12688/openreseurope.19339.3

Bailey, H., Brookes, K. L., and Thompson, P. M. (2014). Assessing environmental impacts of offshore wind farms: lessons learned and recommendations for the future. *Aquat. Biosyst.* 10, 8. doi:10.1186/2046-9063-10-8

Bak, C. (2017). DTU technical report for the DTU 10-MW reference wind turbine. Roskilde, Denmark: Technical University of Denmark (DTU Wind Energy).

Blanco, H., Nijs, W., Ruf, J., and Faaij, A. (2021). Potential of power-to-methane in the eu energy transition. *Appl. Energy* 280, 115943. doi:10.1016/j.apenergy.2020.115943

Borsboom-Hanson, T., Patlolla, S., Herrera, O., and Mérida, W. (2022). Point-to-point transportation: the economics of hydrogen export. *Int. J. Hydrogen Energy* 47, 31541–31550. doi:10.1016/j.ijhydene.2022.07.093

Breyer, C., Bogdanov, D., Aghahosseini, A., Gulagi, A., Child, M., Oyewo, A. S., et al. (2018). Solar photovoltaics demand for the global energy transition in the power sector. *Prog. Photovoltaics Res. Appl.* 26, 505–523. doi:10.1002/pip.2950

Carroll, J., McDonald, A., and McMillan, D. (2015). Failure rate, repair time and unscheduled o&m cost analysis of offshore wind turbines. *Wind Energy* 19, 1107–1119. doi:10.1002/we.1887

Castro-Santos, L., deCastro, M., Costoya, X., Filgueira-Vizoso, A., Lamas, M., Ribeiro, A., et al. (2021). Economic feasibility of floating offshore wind farms considering near future wind resources: case study of iberian coast and bay of biscay. *Int. J. Environ. Res. Public Health* 18, 2553. doi:10.3390/ijerph18052553

Catapult Offshore Renewable Energy (2019). *Guide to an offshore wind farm*. Available online at: https://www.guidetoanoffshorewindfarm.com (Accessed March 18, 2025).

Catapult Offshore Renewable Energy (2023). *Guide to a floating offshore wind farm*. Available online at: https://www.guidetofloatingoffshorewind.com (Accessed January 22, 2025).

Center on Global Energy Policy, Columbia University SIPA (2024). *Demystifying electrolyzer production costs*. Available online at: https://www.energypolicy.columbia.edu/demystifying-electrolyzer-production-costs/ (Accessed December 16, 2024).

Cevasco, D., Koukoura, S., and Kolios, A. (2020). Reliability, availability, maintainability data review for the identification of trends in offshore wind energy applications. *Renew. Sustain. Energy Rev.* 136, 110414. doi:10.1016/j.rser.2020.110414

Chen, Y.-S., Hu, C.-Y., Li, C.-Y., Lin, J.-B., and Shih, Y.-C. (2025). Marine spatial planning for offshore wind firms: a comparison of global existing policies and data for energy system storage. *Sustainability* 17, 5884. doi:10.3390/su17135884

Collin, A. J., Nambiar, A., Bould, D., Whitby, B., Moonem, M., Schenkman, B., et al. (2017). Electrical components for marine renewable energy arrays: a techno-economic review. *Energies* 10, 1973. doi:10.3390/en10121973

Copenhagen Infrastructure Partners (2022). *Hydrogen island (brintØ) — large-scale green hydrogen production project*. Available online at: https://www.cip.com/projects/our-projects/hydrogen-island/ (Accessed January 30, 2026).

Copernicus Climate Change Service (C3S) (2025). *Copernicus european regional reanalysis (cerra)*. Reading, United Kingdom: European Centre for Medium-Range Weather Forecasts (ECMWF).

Copping, A. E., Farr, H., Freeman, M. C., Garavelli, L., Hemery, L. G., Rose, D. J., et al. (2024). OES-environmental 2024 State of the science Report: Environmental effects of marine renewable energy development around the world. *Tech. Rep.* doi:10.2172/2438585

Danish Energy Agency (2024). Technology data for renewable fuels. Available online at: https://ens.dk/en/our-services/technology-catalogues/technology-data-renewable-fuels (Accessed July 25, 2024).

Díaz, H., and Guedes Soares, C. (2023). Cost and financial evaluation model for the design of floating offshore wind farms. *Ocean. Eng.* 287, 115841. doi:10.1016/j.oceaneng.2023.115841

Duan, G., Gattari, D., and Porté-Agel, F. (2025). Theoretical and experimental study on power performance and wake characteristics of a floating wind turbine under pitch motion. *Appl. Energy* 378, 124767. doi:10.1016/j.apenergy.2024.124767

D'Adamo, I., Di Leo, S., Gastaldi, M., Ozturk, I., and Terzi di Bergamo, U. (2025). Exploring the economic feasibility of offshore wind energy for sustainable development. *Energy Rep.* 14, 3093–3104. doi:10.1016/j.egyr.2025.10.003

Elkinton, C. N. (2007). *Offshore wind farm layout optimization*. Amherst, MA, USA: University of Massachusetts. Ph.D. thesis.

EMODnet (2025). Emodnet marine data viewer.

Energy Global (2025). Size matters in offshore wind. Available online at: https://www.energyglobal.com (Accessed March 18, 2025).

EU (2014). Directive 2014/89/EU of the european parliament and of the council of 23 July 2014 establishing a framework for maritime spatial planning. *Official J. Eur. Union L* 257–135.

EU (2023a). Commission delegated regulation (eu) 2023/1184 of 10 February 2023 supplementing directive (eu) 2018/2001 by establishing a union methodology setting out detailed rules for the production of renewable liquid and gaseous transport fuels of non-biological origin. *Official J. Eur. Union*.

EU (2023b). Commission delegated regulation (eu) 2023/1185 of 10 February 2023 supplementing directive (eu) 2018/2001 by establishing a methodology for assessing greenhouse gas emissions savings from renewable liquid and gaseous transport fuels of non-biological origin and from recycled carbon fuels. *Official J. Eur. Union*.

EU (2025). Guidance on eu rules for renewable hydrogen (renewable fuels of non-biological origin). *Eur. Comm.*

European Commission (2012). Orecca: offshore renewable energy conversion and storage infrastructure for countries and regions: final report summary. CORDIS project report.

European Commission (2020a). An EU strategy to harness the potential of offshore renewable energy for a climate neutral future. Brussels, Belgium: European Commission, 741. doi:10.2833/219143

European Commission (2020b). A hydrogen strategy for a climate-neutral Europe. Brussels, Belgium: European Commission, 301.

European Commission (2025a). *European maritime spatial planning platform: introduction to msp*. Brussels, Belgium: European Commission.

European Commission (2025b). *Maestrale: mediterranean alliance for smart energy transition – interreg med*. Brussels, Belgium: European Commission.

European Environment Agency (2025). *Natura2000 data hub*.

Faraggiana, E., Ghigo, A., Sirigu, M., Petracca, E., Giorgi, G., Mattiazzo, G., et al. (2024). Floating offshore wind potential for mediterranean countries. *Heliyon* 10, e33948. doi:10.1016/j.heliyon.2024.e33948

Farahmand, F., King, J., Ghahremanlou, D., Sakthi, P., and Jafari, M. R. M. (2024). A comprehensive systematic overview of canadian hydrogen supply chains downstream. *J. Sustain. Dev.* 17, 1–11. doi:10.5539/jsd.v17n2p1

Gaertner, E., Rinker, J. M., Sethuraman, L., Zahle, F., Anderson, B., Barter, G., et al. (2020). *Definition of the IEA 15-Megawatt offshore reference wind turbine*. Golden, CO,

USA: National Renewable Energy Laboratory NREL. Technical Report NREL/TP-5000-75698.

Gao, Q., Bechlenberg, A., Jayawardhana, B., Ertugrul, N., Vakis, A., and Ding, B. (2024). Techno-economic assessment of offshore wind and hybrid wind–wave farms with energy storage systems. *Renew. Sustain. Energy Rev.* 192, 114263. doi:10.1016/j.rser.2023.114263

GEBCO (2025). Gebco gridded bathymetry data.

Glenk, G., and Reichelstein, S. (2019). Economics of converting renewable power to hydrogen. *Nat. Energy* 4, 216–222. doi:10.1038/s41560-019-0326-1

GME Mercato Elettrico (2025). Report settimanale 40/2025. Available online at: https://gme.mercatoelettrico.org/Portals/0/Documents/it-IT/20251006MGPreportsettimanale40.pdf (Accessed January 30, 2025).

Hill, S. J. P., Bamisile, O., Hatton, L., Staffell, I., and Jansen, M. (2024). The cost of clean hydrogen from offshore wind and electrolysis. *J. Clean. Prod.* 445, 141162. doi:10.1016/j.jclepro.2024.141162

International Energy Agency (2019). Offshore wind outlook 2019: world energy outlook special report. *Tech. Rep.*, 13–15.

International Renewable Energy Agency (2019). Future of wind: deployment, investment, technology, grid integration and socio-economic aspects.

International Renewable Energy Agency (IRENA) (2022). *Geopolitics of the energy transformation: the hydrogen factor*.

Interreg Euro-MED (2025). *Spowind: spatial planning for offshore wind industry development*. Marseille, France: Interreg Euro-MED Programme.

IPCC (2022). *Climate change 2022: mitigation of climate change. contribution of working group iii to the sixth assessment report of the intergovernmental panel on climate change*. Geneva, Switzerland: Intergovernmental Panel on Climate Change (IPCC).

IRENA (2020). Green hydrogen cost reduction: scaling up electrolysers to meet the 1.5°c climate goal. Available online at: https://www.irena.org/publications.Generalreportreference (Accessed November 15, 2025).

Katic, I., Højstrup, J., and Jensen, O. N. (1987). "A simple model for cluster efficiency," in *European Wind Energy Association Conference and Exhibition, EWEC '86 (06–10 Oct 1986)*. Editors W. Palz, and E. Sesto (Rome, Italy: A. Raguzzi), 407–410.

Kaur, N., Hariram, N., Mekha, K., Mohamed, M., Priya, S. S., and Sudhakar, K. (2025). Offshore floating solar with electrofuels for refuelling small ferries: a techno-economic-environmental study. *Energy Convers. Manag. X* 28, 101234. doi:10.1016/j.ecmx.2025.101234

Kumarasamy, S., Selvanathan, S. P., and Ghazali, M. F. (2025). From offshore renewable energy to green hydrogen: addressing critical questions. *Clean. Energy* 9, 108–122. doi:10.1093/ce/zkaf003

Loisel, R., Baranger, L., Chemouri, N., Spinu, S., and Pardo, S. (2015). Economic evaluation of hybrid off-shore wind power and hydrogen storage system. *Int. J. Hydrogen Energy* 40, 6727–6739. doi:10.1016/j.ijhydene.2015.03.117

Maslov, N., Claramunt, C., Wang, T., and Tang, T. (2017). Method to estimate the visual impact of an offshore wind farm. *Appl. Energy* 204, 1422–1430. doi:10.1016/j.apenergy.2017.05.053

MOREnergyLab (2025). Most. Available online at: https://github.com/MOREnergylab/MOST (Accessed November 15, 2025).

Oceanography Center, University of Cyprus (2025). *Thal-chor ii: spatial planning for sustainable aquaculture and blue energy development*.

Onea, F., and Rusu, E. (2022). A spatial analysis of the offshore wind energy potential related to the mediterranean islands. *Energy Rep.* 8, 99–105. doi:10.1016/j.egyr.2022.10.249

Park, S., Lackner, M., Pourazarm, P., Rodriguez Tsouroukdissian, A., and Cross-Whiter, J. (2019). An investigation on the impacts of passive and semiactive structural control on a fixed bottom and a floating offshore wind turbine.

Petracca, E., Issoglio, D., Sirigu, M., Giorgi, G., and Bracco, G. (2024). "Numerical model for 6 DoF dynamics of offshore floating wind turbines," in *A code-to-code comparison between OpenFAST and MOST*, 693–701. doi:10.1201/9781003558859-76

Petracca, E., De Clerck, V., Gorr-Pozzi, E., Mangia, G., Ghigo, A., Joyo, F. H., et al. (2025). "Mediterranean offshore wind: geospatial feasibility for electricity and hydrogen production," in *Proceedings of the SDEWES Conference* (Dubrovnik, Croatia).

Reksten, A. H., Thomassen, M. S., Møller-Holst, S., and Sundseth, K. (2022). Projecting the future cost of pem and alkaline water electrolysers; a capex model including electrolyser plant size and technology development. *Int. J. Hydrogen Energy* 47, 38106–38113. doi:10.1016/j.ijhydene.2022.08.306

Ricchi, A. (2025). Special project progress report 2025: exploiting coupled, high-resolution modelling to simulate severe mediterranean cyclOgenesES (ECHOES). *Tech. Rep.*

Rogeau, A., Vieubled, J., Coatpont, M., Nobrega, P., Erbs, G., and Girard, R. (2023). Techno-economic evaluation and resource assessment of hydrogen production through offshore wind farms: a European perspective. *Renew. Sustain. Energy Rev.* 187. doi:10.1016/j.rser.2023.113699

Sakthi, P., and Ghahremanlou, D. (2024). A systematic review and bibliometric analysis of sustainable hydrogen production and distribution in Canada. *J. Green Econ. Low-Carbon Dev.* 3, 132–160. doi:10.56578/jgelcd030301

Santos, V., Elizetxea-Navarro, A., Blanco-Aguilera, R., Peña Sanchez, Y., Goikoetxea, A., and Penalba, M. (2024). Green hydrogen production in offshore wind farms: centralised vs. decentralised, 915–922. doi:10.1201/9781003558859-99

Singlitico, A., Østergaard, J., and Chatzivasileiadis, S. (2021). Onshore, offshore or in-turbine electrolysis? Techno-economic overview of alternative integration designs for green hydrogen production into offshore wind power hubs. *Renew. Sustain. Energy Transition* 1, 100005. doi:10.1016/j.rset.2021.100005

Soukissian, T., Karathanasi, F., Axaopoulos, P., Voukouvalas, E., and Kotroni, V. (2017). Offshore wind climate analysis and variability in the mediterranean sea. *Int. J. Climatol.* 38, 384–402. doi:10.1002/joc.5182

SPOWIND Consortium (2025a). Power-to-X technologies and opportunities. *Tech. Rep. Deliv. D3.2.1, SPOWIND – Spatial Plan. Offshore WIND Industry Dev. Interreg. Euro-MED. Intern. Project Report*.

SPOWIND Consortium (2025b). Techno-economic assessment methods for offshore wind farms. *Tech. Rep. Deliv. D2.3.1, SPOWIND – Spatial Plan. Offshore WIND Industry Dev. Interreg. Euro-MED. Intern. Project Report*.

Stehly, T., Beiter, P., and Duffy, P. (2020). NREL 2019 cost of wind energy review. *Tech. Rep.*, 77.

Timalsina, D., and Ghahremanlou, D. (2024). Optimizing wind-to-hydrogen production in newfoundland for export: a techno-economic perspective. *Eur. J. Energy Res.* 4, 28–35. doi:10.24018/ejenergy.2024.4.2.139

United Nations Global Compact (2021). *Roadmap to integrate clean offshore renewable energy into climate-smart marine spatial planning. Report*. New York, United States: United Nations Global Cmpact Office.

U.S. Department of Energy, Office of Clean Energy Demonstrations (2026). *Regional clean hydrogen hubs*. Available online at: https://www.energy.gov/oced/regional-clean-hydrogen-hubs-0 (Accessed January 30, 2026).

Vieira, M. (2020). *Viability of structural health monitoring systems on the support structures of offshore wind turbines*. Universidade de Lisboa: Instituto Superior Técnico. Ph.D. thesis.

WestMED Initiative (2023). *Pelagos initiative forum 2023. Event summary, online*.

Younus, H. A., Al Hajri, R., Ahmad, N., Al-Jammal, N., Verpoort, F., and Al Abri, M. (2025). Green hydrogen production and deployment: opportunities and challenges. *Discov. Electrochem.* 2, 32. doi:10.1007/s44373-025-00043-9

Zaiter, Y., Lago, M., Maund, J., van Duinen, R., Chouchane, H., van den Burg, S. W. K., et al. (2025). Investigating levies and barriers for the development of offshore multi-use platforms in european regional seas. *Front. Ocean Sustain.* 3, 1542309. doi:10.3389/focsu.2025.1542309